

Formation of interference patterns in diffusively scattered fields at a double-exposure recording of quasi-Fourier and Fourier holograms using a Galilean telescope

V.G. Gusev

Tomsk State University

Received November 6, 2007

The sensitivity of the interferometer to transversal or longitudinal displacements of a plate surface diffusively scattering light is analyzed. It is shown that interference patterns are located in the hologram and Fourier planes. Spatial filtration of the diffraction field is required. The experimental results agree well with theoretical prerequisites.

When controlling the transversal displacement of a flat surface (as it was shown in Ref. 1) diffusively scattering light (hereinafter scatterer), at a double-exposure recording with a Kepler tube of the hologram of the focused scatterer image, the interference patterns are localized in the hologram plane and in far diffraction zone. In the case of interference pattern localization in the hologram plane, the interferometer sensitivity linearly depends on the telescope magnification and is independent of the curvature of a spherical wave of the coherent radiation, used to illuminate the scatterer when recording the hologram. For the interference pattern, localized in the Fourier plane, the interferometer sensitivity depends on the focal length of the telescopic lens.

When controlling longitudinal displacement of the scatterer, the interferometer sensitivity for an interference pattern, localized in the hologram plane, is in squared relationship with the telescope magnification and independent of the curvature of a spherical wave of the coherent radiation, used to illuminate the scatterer when recording the hologram. For an interference pattern, localized in the Fourier plane, the interferometer sensitivity is in squared relationship with the focal length of the telescopic lens of the Kepler tube. In addition, the center of the system of concentric interference rings, characterizing longitudinal displacement of the scatterer, is fixed while carrying out the spatial filtration of the off-axis diffraction field both in the hologram and Fourier planes.

In this work, peculiarities of formation of interference patterns are analyzed, which characterize transversal or longitudinal displacements of the scatterer at a double-exposure recording of the quasi-Fourier and Fourier holograms with the use of a Galilean telescope in order to determine the interferometer sensitivity.

In Fig. 1 the opaque screen 1 in the plane (x_1, y_1) is illuminated by coherent radiation with divergent spherical wave of the curvature radius R . Radiation, diffusively scattered by the screen and passing the

microscope optics of the Galilean telescope (positive thin lens L_1 is the objective and negative thin lens L_2 is the ocular), is recorded during the first exposure on the photoplate 2 in the plane (x_4, y_4) by means of the off-axis reference spherical wave of the curvature r ; θ is the angle between the axis of a spatially limited reference beam with the normal to the photoplate plane. Before the second exposure, the opaque screen is displaced in its plane, e.g., by α toward the x -axis.

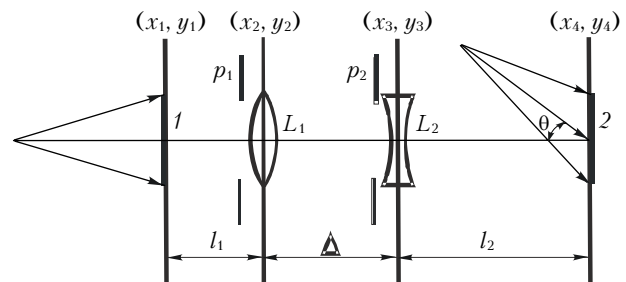


Fig. 1. Schematic view of the two-exposure hologram recording: 1 is the opaque screen; 2 is the photoplate; L_1 is the positive and L_2 is the negative lens; p_1 and p_2 are the objective apertures.

Write the distribution of the field complex amplitude, corresponding to the first exposure, to the Fresnel approximation with accounting for the diffraction limitedness, in the object channel in the photoplate plane in the form

$$u_1(x_4, y_4) \sim \iiint \int_{-\infty}^{\infty} t(x_1, y_1) \exp\left[\frac{ik}{2R}(x_1^2 + y_1^2)\right] \times \\ \times \exp\left\{\frac{ik}{2l_1}[(x_1 - x_2)^2 + (y_1 - y_2)^2]\right\} p_1(x_2, y_2) \times \\ \times \exp\left[-\frac{ik}{2f_1}(x_2^2 + y_2^2)\right] \exp\left\{\frac{ik}{2\Delta}[(x_2 - x_3)^2 + (y_2 - y_3)^2]\right\} \times$$

$$\begin{aligned} & \times p_2(x_3, y_3) \exp\left[\frac{ik}{2f_2}(x_3^2 + y_3^2)\right] \times \\ & \times \exp\left\{\frac{ik}{2l_2}[(x_3 - x_4)^2 + (y_3 - y_4)^2]\right\} dx_1 dy_1 dx_2 dy_2 dx_3 dy_3, \end{aligned} \tag{1}$$

where k is the wave number; $t(x_1, y_1)$ is the complex amplitude of the scatterer transmittance, being the random function of coordinates; f_1 is the focal length of the positive lens L_1 with the pupil function $p_1(x_2, y_2)$ [Ref. 2]; f_2 is the focal length of the negative lens L_2 with the pupil function $p_2(x_3, y_3)$; $\Delta = f_1 - f_2$ is the microscope tube length; l_1 and l_2 are the distances between the planes (x_1, y_1) , (x_2, y_2) and (x_3, y_3) , (x_4, y_4) , respectively; (x_2, y_2) and (x_3, y_3) are the principal planes of the lens L_1 and L_2 .

Similar to Refs. 3 and 4, equation (1) can be represented with the convolutions of functions, i.e.,

$$\begin{aligned} u_1(x_4, y_4) \sim & \exp\left[\frac{ik}{2l_2}(x_4^2 + y_4^2)\right] \left\{ \exp\left[-\frac{ikL_1}{2l_1^2}(x_4^2 + y_4^2)\right] \times \right. \\ & \times \left\{ \exp\left[-\frac{ikL_1^2 L_2}{2l_2^2 \Delta^2}(x_4^2 + y_4^2)\right] \int_{-\infty}^{\infty} \int_{-\infty}^{\infty} t(x_1, y_1) \times \right. \\ & \times \exp\left[\frac{ik(R+l_1)}{2Rl_1}(x_1^2 + y_1^2)\right] \exp\left[-\frac{ikL_2}{2l_1^2}(x_1^2 + y_1^2)\right] \times \\ & \times \exp\left[-\frac{ikL_1 L_2}{l_1 l_2 \Delta}(x_1 x_4 + y_1 y_4)\right] dx_1 dy_1 \otimes P_1(x_4, y_4) \left. \right\} \otimes \\ & \left. \otimes P_2(x_4, y_4) \right\}, \end{aligned} \tag{2}$$

where \otimes denotes the convolution; $(1/L_1) = 1/\Delta + 1/f_2 + 1/l_2$; $(1/L_2) = 1/l_1 - 1/f_1 + 1/\Delta - L_1/\Delta^2$ are the contractions; $P_1(x_4, y_4)$ is the Fourier transform of $p_1(x_2, y_2)$ with the spatial frequencies $L_1 x_4/\lambda l_2 \Delta$ and $L_1 y_4/\lambda l_2 \Delta$ (λ is the wavelength of the coherent light source, used for hologram recording and retrieval); $P_2(x_4, y_4)$ is the Fourier transform of $p_2(x_3, y_3)$ with the spatial frequencies $x_4/\lambda l_2$ and $y_4/\lambda l_2$.

Let the width of the function $P_1(x_4, y_4)$ be about $\lambda l_2 \Delta/d_1 L_1$,⁵ where d_1 is the pupil function of the lens L_1 (see Fig. 1). If the phase change of a spherical wave with the curvature $l_2^2 \Delta^2/L_1^2 L_2$ does not exceed π within the domain of $P_1(x_4, y_4)$ existence, this condition is to fulfill in the plane (x_4, y_4) for an area of the diameter $D_1 \leq d_1 l_2 \Delta/L_1 L_2$. Then take the factor $\exp[-ikL_1^2 L_2(x_4^2 + y_4^2)/2l_2^2 \Delta^2]$ out of the integral of convolution with $P_1(x_4, y_4)$ in Eq. (2) and obtain

$$\begin{aligned} u_1(x_4, y_4) \sim & \exp\left[\frac{ik}{2l_2}(x_4^2 + y_4^2)\right] \times \\ & \times \left\{ \exp\left[-\frac{ik(L_1 \Delta^2 + L_1^2 L_2)}{2l_2^2 \Delta^2}(x_4^2 + y_4^2)\right] \times \right. \end{aligned}$$

$$\begin{aligned} & \times \left\{ \int_{-\infty}^{\infty} \int_{-\infty}^{\infty} t(x_1, y_1) \exp\left[\frac{ik(R+l_1)}{2Rl_1}(x_1^2 + y_1^2)\right] \times \right. \\ & \times \exp\left[-\frac{ikL_2}{2l_1^2}(x_1^2 + y_1^2)\right] \exp\left[-\frac{ikL_1 L_2}{l_1 l_2 \Delta}(x_1 x_4 + y_1 y_4)\right] \times \\ & \left. \left. \times dx_1 dy_1 \otimes P_1(x_4, y_4) \right\} \otimes P_2(x_4, y_4) \right\}. \end{aligned} \tag{3}$$

The width of $P_2(x_4, y_4)$ is about $\lambda l_2/d_2$ (d_2 is the pupil function of the lens L_2); therefore, within the domain of the function existence, the phase change of a spherical wave with the curvature $l_2^2 \Delta^2/(L_1 \Delta^2 + L_1^2 L_2)$ does not exceed π for an area of $D_2 \leq d_2 l_2 \Delta^2/(L_1 \Delta^2 + L_1^2 L_2)$ in diameter in the plane (x_4, y_4) . Then, take the factor $\exp[-ik(L_1 \Delta^2 + L_1^2 L_2)(x_4^2 + y_4^2)/2l_1^2 \Delta^2]$ out of the integral of convolution with $P_2(x_4, y_4)$ in Eq. (3). Besides, if $d_1 = \mu d_2$ ($\mu = f_1/f_2$ is the magnification of the Galilean telescope), then, with accounting for $L_1 = l_2 \Delta/(\mu l_2 + \Delta)$ and $L_2 = l_1(\mu l_2 + \Delta)/\mu l$, where $l = l_2 + \Delta/\mu + l_1/\mu^2$, the distribution of the field complex amplitude in the object channel in the photoplate plane for an area of $D \leq d_1 l(\mu l_2 + \Delta)/(l_1 l_2 + \mu l \Delta)$ in diameter takes the form

$$\begin{aligned} u_1(x_4, y_4) \sim & \exp\left[\frac{ik}{2r}(x_4^2 + y_4^2)\right] \times \\ & \times \left\{ F(x_4, y_4) \otimes \exp\left[-\frac{ikR}{2l(R+\mu^2 l)}(x_4^2 + y_4^2)\right] \otimes \right. \\ & \left. \otimes P_1(x_4, y_4) \otimes P_2(x_4, y_4) \right\}, \end{aligned} \tag{4}$$

where $r = l$; $F(x_4, y_4)$ is the Fourier transform of $t(x_1, y_1)$ with the spatial frequencies $x_4/\lambda \mu l$ and $y_4/\lambda \mu l$; $P_1(x_4, y_4)$ is the Fourier transform of $p_1(x_2, y_2)$ with the spatial frequencies $x_4/\lambda(\mu l_2 + \Delta)$ and $y_4/\lambda(\mu l_2 + \Delta)$.

It follows from Eq. (4), that the quasi-Fourier transform of the transmission function of opaque screen 1 is formed in the plane of photoplate 2 (see Fig. 1) within the above area. In this case, each point of the screen is extended up to the size of the subjective speckle, defined by the width of the function $P_1(x_4, y_4) \otimes P_2(x_4, y_4)$; and the distribution of the phase of a divergent spherical wave with the curvature l is superimposed on the subjective speckle field. In the special case of scatterer illumination by coherent radiation with a convergent spherical wave of the curvature $\mu^2 l$, the distribution of the field complex amplitude in the plane (x_4, y_4) corresponds to the Fourier transform of $t(x_1, y_1)$.

The distribution of the complex amplitude of the field, corresponding to the second exposure, in the object channel in the photoplate plane is defined by the equation (to the used approximation)

$$\begin{aligned}
 u_2(x_4, y_4) \sim & \iiint \iiint_{-\infty}^{\infty} t(x_1 + a, y_1) \exp\left[\frac{ik}{2R}(x_1^2 + y_1^2)\right] \times \\
 & \times \exp\left\{\frac{ik}{2l_1}[(x_1 - x_2)^2 + (y_1 - y_2)^2]\right\} p_1(x_2, y_2) \times \\
 & \times \exp\left[-\frac{ik}{2f_1}(x_2^2 + y_2^2)\right] \exp\left\{\frac{ik}{2\Delta}[(x_2 - x_3)^2 + (y_2 - y_3)^2]\right\} \times \\
 & \times p_2(x_3, y_3) \exp\left[\frac{ik}{2f_2}(x_3^2 + y_3^2)\right] \times \\
 & \times \exp\left\{\frac{ik}{2l_2}[(x_3 - x_4)^2 + (y_3 - y_4)^2]\right\} dx_1 dy_1 dx_2 dy_2 dx_3 dy_3.
 \end{aligned} \tag{5}$$

With accounting for the Fourier transform properties and the known identity,³ equation (5) takes the form

$$\begin{aligned}
 u_2(x_4, y_4) \sim & \exp\left[\frac{ik}{2l_2}(x_4^2 + y_4^2)\right] \times \\
 & \times \left\{ \exp\left[-\frac{ik(L_1\Delta^2 + L_1^2L_2)}{2l_2^2\Delta^2}(x_4^2 + y_4^2)\right] \exp\left(\frac{ikax_4}{\mu l}\right) \times \right. \\
 & \times \left. \left\{ F(x_4, y_4) \otimes \exp\left(-\frac{ikax_4}{\mu l}\right) \exp\left[-\frac{ikR}{2l(R + \mu^2l)}(x_4^2 + y_4^2)\right] \otimes \right. \right. \\
 & \left. \left. \otimes \exp\left(-\frac{ikax_4}{\mu l}\right) P_1(x_4, y_4) \right\} \otimes P_2(x_4, y_4) \right\}.
 \end{aligned} \tag{6}$$

Since

$$\begin{aligned}
 & \exp\left[-ikR(x_4^2 + y_4^2)/2l(R + \mu^2l)\right] \otimes \\
 & \otimes \exp\left[ikR(x_4^2 + y_4^2)/2l(R + \mu^2l)\right] = \delta(x_4, y_4)
 \end{aligned}$$

(see, e.g., Ref. 6, where $\delta(x_4, y_4)$ is the Dirac delta function), the proof of the identity

$$\begin{aligned}
 & \exp\left[\frac{ikR}{2l(R + \mu^2l)}(x_4^2 + y_4^2)\right] \otimes \exp\left(-\frac{ikax_4}{\mu l}\right) \times \\
 & \times \exp\left[-\frac{ikR}{2l(R + \mu^2l)}(x_4^2 + y_4^2)\right] \otimes \exp\left(-\frac{ikax_4}{\mu l}\right) P_1(x_4, y_4) = \\
 & = \exp\left[-\frac{ik(R + \mu^2l)a^2}{2\mu^2Rl}\right] \exp\left(-\frac{ikax_4}{\mu l}\right) \times \\
 & \times P_1\left[x_4 + \frac{a(R + \mu^2l)}{\mu R}, y_4\right]
 \end{aligned} \tag{7}$$

follows from the integral representation of convolution operation in Eq. (6). Hence, the distribution of the complex amplitude of the field, corresponding to the second exposure, in the object channel in the photoplate plane within the above area takes the form

$$\begin{aligned}
 u_2(x_4, y_4) \sim & \exp\left[-\frac{ik(R + \mu^2l)a^2}{2\mu^2Rl}\right] \times \\
 & \times \exp\left(\frac{ikax_4}{\mu l}\right) \exp\left[\frac{ik}{2r}(x_4^2 + y_4^2)\right] \times \\
 & \times \left\{ F(x_4, y_4) \otimes \exp\left[-\frac{ikR}{2l(R + \mu^2l)}(x_4^2 + y_4^2)\right] \otimes \exp\left(-\frac{ikax_4}{\mu l}\right) \times \right. \\
 & \left. \times \left\{ P_1\left[x_4 + \frac{a(R + \mu^2l)}{\mu R}, y_4\right] \otimes P_2(x_4, y_4) \right\} \right\}.
 \end{aligned} \tag{8}$$

According to Eq. (8), the transversal displacement of the scatterer is accompanied by variation of a slope angle of the subjective speckle-field, corresponding to the second exposure, by $a/\mu l$ relative to the speckle-field of the first exposure. In addition, the subjective speckle component, caused by the diffraction of a plane wave on the Galilean telescope objective pupil, is homogeneously displaced to $(R + \mu^2l)a/\mu R$. In this case, the displacement direction depends on the sign of the curvature R . This follows from the fact that the Fourier transform of $t(x_1, y_1)$ is formed in the photoplate plane for negative R , equal in modulus to μ^2l . In this case, displacement of the above subjective speckle component is absent. However, displacement in opposite directions takes place at $R < \mu^2l$ and $R > \mu^2l$. In its turn, the displacement for positive R is co-directed with those of the scatterer.

If the quasi-Fourier or Fourier hologram is double-exposure recorded with a convergent reference spherical wave with the curvature $r = l$ at the linear part of the photo-material blackening curve, then the distribution of the complex amplitude of its transmittance, corresponding to the (-1) -st diffraction order, on the base of Eqs. (4) and (8) is defined by the equation

$$\begin{aligned}
 \tau(x_4, y_4) \sim & \exp(-ikx_4 \sin\theta) \left\{ F(x_4, y_4) \otimes \right. \\
 & \otimes \exp\left[-\frac{ikR}{2l(R + \mu^2l)}(x_4^2 + y_4^2)\right] \otimes P_1(x_4, y_4) \otimes P_2(x_4, y_4) + \\
 & + \exp\left[-\frac{ik(R + \mu^2l)a^2}{2\mu^2Rl}\right] \exp\left(\frac{ikax_4}{\mu l}\right) \times \\
 & \times \left\{ F(x_4, y_4) \otimes \exp\left[-\frac{ikR}{2l(R + \mu^2l)}(x_4^2 + y_4^2)\right] \otimes \right. \\
 & \left. \left. \otimes \exp\left(-\frac{ikax_4}{\mu l}\right) \left\{ P_1\left[x_4 + \frac{(R + \mu^2l)a}{\mu R}, y_4\right] \otimes P_2(x_4, y_4) \right\} \right\} \right\}.
 \end{aligned} \tag{9}$$

Let the diffraction field be spatially filtered at retrieving the double-exposure hologram in the its

plane on the optical axis with a round aperture in the opaque screen p_0 (Fig. 2).

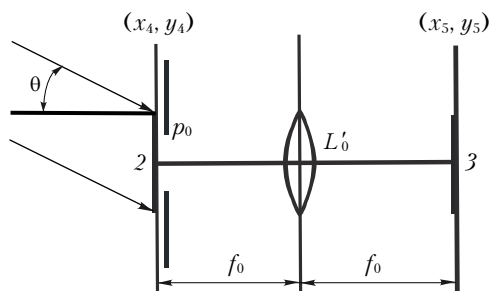


Fig. 2. Schematic view of recording of the interference pattern localized in the scatterer-imaging plane: hologram 2; recording plane 3; positive lens L'_0 ; spatial filter p_0 .

In this case, within the filtering aperture diameter, the phase change $kax_4/\mu l$ does not exceed π . Then the distribution of the field complex amplitude at the spatial filter outlet is defined as

$$\begin{aligned}
 u(x_4, y_4) &\sim p_0(x_4, y_4) \times \\
 &\times \left\{ F(x_4, y_4) \otimes \exp \left[-\frac{ikR}{2l(R + \mu^2 l)} (x_4^2 + y_4^2) \right] \otimes \right. \\
 &\otimes P_1(x_4, y_4) \otimes P_2(x_4, y_4) + \exp \left[-\frac{ik(R + \mu^2 l)}{2\mu^2 R l} a^2 \right] \left\{ F(x_4, y_4) \otimes \right. \\
 &\otimes \exp \left[-\frac{ikR}{2l(R + \mu^2 l)} (x_4^2 + y_4^2) \right] \otimes \exp \left(-\frac{ikax_4}{\mu l} \right) \times \\
 &\times \left. \left. \left. \left. P_1 \left(x_4 + \frac{(R + \mu^2 l)}{\mu R} a, y_4 \right) \otimes P_2(x_4, y_4) \right) \right) \right\} \right\}, \quad (10)
 \end{aligned}$$

where $p_0(x_4, y_4)$ is the transmission function of the opaque screen with a round aperture.⁷

Based on Eq. (10) and with accounting for parity of the functions $p_1(x_2, y_2)$ and $p_2(x_3, y_3)$, the distribution of the field complex amplitude in the back focal plane of the lens L'_0 (see Fig. 2) with the focal length f_0 is defined by the equation

$$\begin{aligned}
 u(x_5, y_5) &\sim \left\{ p_1 \left(\frac{\Delta + \mu l_2}{f_0} x_5, \frac{\Delta + \mu l_2}{f_0} y_5 \right) p_2 \left(\frac{l_2}{f_0} x_5, \frac{l_2}{f_0} y_5 \right) \times \right. \\
 &\times t \left(-\frac{\mu l}{f_0} x_5, -\frac{\mu l}{f_0} y_5 \right) \exp \left[\frac{ikl(R + \mu^2 l)}{2Rf_0^2} (x_5^2 + y_5^2) \right] + \\
 &+ \exp \left[\frac{ik(R + \mu^2 l)a^2}{2\mu^2 R l} \right] \exp \left[\frac{ik(R + \mu^2 l)}{\mu R f_0} ax_5 \right] \times \\
 &\times p_1 \left(\frac{\Delta + \mu l_2}{f_0} x_5 + \frac{\Delta + \mu l_2}{\mu l} a, \frac{\Delta + \mu l_2}{f_0} y_5 \right) \times \\
 &\times p_2 \left(\frac{l_2}{f_0} x_5 + \frac{l_2}{\mu l} a, \frac{l_2}{f_0} y_5 \right) t \left(-\frac{\mu l}{f_0} x_5, -\frac{\mu l}{f_0} y_5 \right) \times
 \end{aligned}$$

$$\times \exp \left[\frac{ikl(R + \mu^2 l)}{2Rf_0^2} (x_5^2 + y_5^2) \right] \otimes P_0(x_5, y_5), \quad (11)$$

where $P_0(x_5, y_5)$ is the Fourier transform of $p_0(x_4, y_4)$ with the spatial frequencies $x_5/\lambda f_0$ and $y_5/\lambda f_0$.

If the variation period of $1 + \exp[ik(R + \mu^2 l)a^2/2\mu^2 R l] \times \exp[ik(R + \mu^2 l)ax_5/\mu R f_0]$ is at least an order of magnitude⁹ larger than the width of $P_0(x_5, y_5)$, determining the size of subjective speckle in hologram recording plane 3 (see Fig. 2), within limits of overlap of the functions $p_1[(\Delta + \mu l_2)x_5/f_0, (\Delta + \mu l_2)y_5/f_0] p_2(l_2 x_5/f_0, l_2 y_5/f_0)$, $p_1[(\Delta + \mu l_2)x_5/f_0 + (\Delta + \mu l_2)a/\mu l, (\Delta + \mu l_2)y_5/f_0] p_2(l_2 x_5/f_0 + l_2 a/\mu l, l_2 y_5/f_0)$, where the field is non-zero, then we take it out of the convolution integral in Eq. (11). Again, with accounting for smallness of $(\Delta + \mu l_2)a/\mu l$ and $l_2 a/\mu l$, the light distribution in the plane (x_5, y_5) has the form

$$\begin{aligned}
 I(x_5, y_5) &\sim \left\{ 1 + \cos \left(\frac{k(R + \mu^2 l)a^2}{2\mu^2 R l} + \frac{k(R + \mu^2 l)}{\mu R f_0} ax_5 \right) \right\} \times \\
 &\times \left| p_1 \left(\frac{\Delta + \mu l_2}{f_0} x_5, \frac{\Delta + \mu l_2}{f_0} y_5 \right) p_2 \left(\frac{l_2}{f_0} x_5, \frac{l_2}{f_0} y_5 \right) t \left(-\frac{\mu l}{f_0} x_5, -\frac{\mu l}{f_0} y_5 \right) \times \right. \\
 &\times \left. \exp \left[\frac{ikl(R + \mu^2 l)}{2Rf_0^2} (x_5^2 + y_5^2) \right] \otimes P_0(x_5, y_5) \right|^2. \quad (12)
 \end{aligned}$$

It follows from Eq. (12) that the diameter D_0 of the illuminated area of the opaque screen (see Fig. 1) is to satisfy the condition $D_0 \geq d_1 \mu l / (\Delta + \mu l_2)$ for diffraction boundedness of the Galilean telescope's field of view. Besides, the subjective speckle structure is modulated by fringes, alternate on the x -axis, in the far focal plane of the lens L'_0 (see Fig. 2), where a scatterer image is forming within the diameter of the telescope pupil (since $l_2 < (\Delta + \mu l_2)/\mu$).

The measurement of the fringe period for the known λ, μ, R, l , and f_0 allows controlling the transversal displacement of the scatterer. In this case, the sensitivity of the interferometer depends both on the value and sign of curvature of a spherical wave of the coherent radiation, used to illuminate the scatterer while recording the hologram. Thus, for a positive R , the fringe period $\Delta x_5 = \lambda \mu R f_0 / (R + \mu^2 l) a$ decreases with decreasing R due to an increase of displacement of the above component of the subjective speckle, corresponding to the second exposure, in the hologram plane.

When opaque screen 1 (see Fig. 1) is illuminated with coherent radiation with convergent spherical waves, the fringe period increases with decreasing R within a range $\mu^2 l \leq R \leq \infty$ up to infinity when $R = \mu^2 l$, and the Fourier transform of the function $t(x_1, y_1)$ is formed in the hologram plane. In this case, the speckles, corresponding to the second exposure, are static. A further decrease of R results in interferometer sensitivity enhancement at recording of the interference

pattern, localized in the scatterer-imaging plane, due to occurrence and increase of a homogeneous displacement of the subjective speckle component, caused by the diffraction of a plane wave on the pupil of Galilean telescope, in the hologram plane. It also follows from Eq. (12) that the spatial extension of the interference pattern $s = d_1 f_0 / (\mu l_2 + \Delta)$ in the Fourier plane.

Consider spatial filtration of the diffraction field on the optical axis in the scatterer-imaging plane (x_5, y_5) at the stage of retrieving the double-exposure quasi-Fourier hologram (Fig. 3). Assume, for brevity, that hereinafter the focal lengths f_{01} and f_{02} of the lenses L'_0 and L''_0 are equal to f_0 , i.e., the two-component optical system of the positive lenses L'_0 and L''_0 forms the hologram image in the plane (x_6, y_6) with the unity magnification.

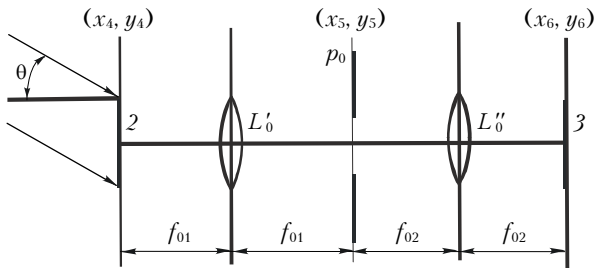


Fig. 3. Schematic view of recording of the interference pattern, localizing in the hologram plane: hologram 2; recording plane 3; positive lenses L'_0 and L''_0 ; spatial filter p_0 .

In this case, based on the integral convolution representation, define the distribution of the field complex amplitude at the hologram output as

$$\begin{aligned}
 u(x_4, y_4) \sim & \exp\left[-\frac{ikR}{2l(R + \mu^2 l)}(x_4^2 + y_4^2)\right] \times \\
 & \times \left\{ \exp\left[\frac{ikR}{2l(R + \mu^2 l)}(x_4^2 + y_4^2)\right] \otimes t\left(\frac{\mu R}{R + \mu^2 l}x_4, \frac{\mu R}{R + \mu^2 l}y_4\right) \right\} \otimes \\
 & \otimes P_1(x_4, y_4) \otimes P_2(x_4, y_4) + \exp\left[-\frac{ik(R + \mu^2 l)}{2\mu^2 R l}a^2\right] \times \\
 & \times \exp\left(\frac{ikax_4}{\mu l}\right) \left\{ \exp\left[-\frac{ikR}{2l(R + \mu^2 l)}(x_4^2 + y_4^2)\right] \times \right. \\
 & \times \left. \left\{ \exp\left[\frac{ikR}{2l(R + \mu^2 l)}(x_4^2 + y_4^2)\right] \otimes t\left(\frac{\mu R}{R + \mu^2 l}x_4, \frac{\mu R}{R + \mu^2 l}y_4\right) \right\} \otimes \right. \\
 & \left. \otimes \exp\left(-\frac{ikax_4}{\mu l}\right) \left\{ P_1\left[x_4 + \frac{R + \mu^2 l}{\mu R}a^2, y_4\right] \otimes P_2(x_4, y_4) \right\} \right\}. \quad (13)
 \end{aligned}$$

Hence, neglecting the spatial boundedness of the field due to finite sizes of the hologram and lens L'_0 (see Fig. 3), define the distribution of its complex amplitude in the plane (x_5, y_5) by the equation

$$\begin{aligned}
 u(x_5, y_5) \sim & p_1\left(\frac{\Delta + \mu l_2}{f_0}x_5, \frac{\Delta + \mu l_2}{f_0}y_5\right) \times \\
 & \times p_2\left(\frac{l_2}{f_0}x_5, \frac{l_2}{f_0}y_5\right) \left\{ \exp\left[\frac{ikl(R + \mu^2 l)}{2Rf_0^2}(x_5^2 + y_5^2)\right] \right\} \otimes \\
 & \otimes F_1(x_5, y_5) \exp\left[-\frac{ikl(R + \mu^2 l)}{2Rf_0^2}(x_5^2 + y_5^2)\right] + \\
 & + \exp\left[\frac{ik(R + \mu^2 l)}{2\mu^2 R l}a^2\right] \exp\left[\frac{ik(R + \mu^2 l)}{\mu R f_0}ax_5\right] \times \\
 & \times p_1\left(\frac{\Delta + \mu l_2}{f_0}x_5 + \frac{\Delta + \mu l_2}{\mu l}a, \frac{\Delta + \mu l_2}{f_0}y_5\right) p_2\left(\frac{l_2}{f_0}x_5 + \frac{l_2}{\mu l}a, \frac{l_2}{f_0}y_5\right) \times \\
 & \times \left\{ \exp\left[\frac{ikl(R + \mu^2 l)}{2Rf_0^2}\left[\left(x_5 - \frac{f_0}{\mu l}a\right)^2 + y_5^2\right]\right] \right\} \otimes \\
 & \otimes F_1(x_5, y_5) \exp\left[-\frac{ikl(R + \mu^2 l)}{2Rf_0^2}(x_5^2 + y_5^2)\right] \left. \right\}, \quad (14)
 \end{aligned}$$

where $F_1(x_5, y_5)$ is the Fourier transform of the function $t[\mu R \xi / (R + \mu^2 l), \mu R \eta / (R + \mu^2 l)]$ with the spatial frequencies $x_5 / \lambda f_0$ and $y_5 / \lambda f_0$.

If the phase change $[k(R + \mu^2 l)ax_5 / \mu R f_0] \leq \pi$ within the diameter of the filtering aperture of the spatial filter p_0 (see Fig. 3), then the distribution of the field complex amplitude at its outlet takes the form

$$\begin{aligned}
 u(x_5, y_5) \sim & p_0(x_5, y_5) \left\{ \exp\left[\frac{ikl(R + \mu^2 l)}{2Rf_0^2}(x_5^2 + y_5^2)\right] \right\} \otimes \\
 & \otimes F_1(x_5, y_5) \exp\left[-\frac{ikl(R + \mu^2 l)}{2Rf_0^2}(x_5^2 + y_5^2)\right] + \\
 & + \exp\left[\frac{ik(R + \mu^2 l)}{2\mu^2 R l}a^2\right] \exp\left[\frac{ikl(R + \mu^2 l)}{2Rf_0^2}\left[\left(x_5 - \frac{f_0}{\mu l}a\right)^2 + y_5^2\right]\right] \otimes \\
 & \otimes F_1(x_5, y_5) \exp\left[-\frac{ikl(R + \mu^2 l)}{2Rf_0^2}(x_5^2 + y_5^2)\right] \left. \right\}, \quad (15)
 \end{aligned}$$

where $p_0(x_5, y_5)$ is the transmission function of the spatial filter.

Hence, after the Fourier transform, the distribution of the field complex amplitude in the plane (x_6, y_6) (see Fig. 3) is defined as

$$\begin{aligned}
 u(x_6, y_6) \sim & \left\{ \left\{ 1 + \exp\left[\frac{ik(R + \mu^2 l)a^2}{2\mu^2 R l}\right] \exp\left(-\frac{ikax_6}{\mu l}\right) \right\} \times \right. \\
 & \times \exp\left[-\frac{ikR}{2l(R + \mu^2 l)}(x_6^2 + y_6^2)\right] \times \\
 & \left. \times \left\{ t\left(-\frac{\mu R}{R + \mu^2 l}x_6, -\frac{\mu R}{R + \mu^2 l}y_6\right) \right\} \right\}
 \end{aligned}$$

$$\otimes \exp \left[\frac{ikR}{2l(R + \mu^2 l)} (x_6^2 + y_6^2) \right] \otimes P_0(x_6, y_6), \quad (16)$$

where $P_0(x_6, y_6)$ is the Fourier transform of $p_0(x_5, y_5)$ with the spatial frequencies $x_6/\lambda f_0$ and $y_6/\lambda f_0$.

If the variation period of $1 + \exp[ik(R + \mu^2 l)a^2/2\mu^2 Rl] \exp(-ikax_6/\mu l)$ is at least an order of magnitude larger than the width of $P_0(x_6, y_6)$, determining the size of subjective speckle in recording plane 3 (see Fig. 3), then take it out of the integral of convolution in Eq. (16). Then, using the integral convolution representation, write the light distribution in the plane (x_6, y_6) in the form

$$I(x_6, y_6) \sim \left\{ 1 + \cos \left[\frac{k(R + \mu^2 l)}{2\mu^2 Rl} a^2 - \frac{kax_6}{\mu l} \right] \right\} \times \\ \times \left| F(-x_6, -y_6) \otimes \exp \left[-\frac{ikR}{2l(R + \mu^2 l)} (x_6^2 + y_6^2) \right] \otimes \right. \\ \left. \otimes P_0(x_6, y_6) \right|^2. \quad (17)$$

It follows from Eq. (17) that the interference pattern in the form of fringes, alternating on the x -axis, is formed, modulating the subjective speckle structure, when imaging a hologram with the use of Kepler tube with spatial filtration of the diffraction field in its frequency plane. In this case, the fringe period $\Delta x_6 = \lambda \mu l / a$ is independent of the curvature of a spherical wave of the coherent radiation, used to illuminate the scatterer while recording the hologram, and decreases with a decrease of the scale of the Fourier transform of the function, characterizing the complex amplitude of scatterer transmittance or reflection, in the hologram plane. Besides, if the diameters of the collimated beam, retrieving the hologram, and of the lens L'_0 (see Fig. 3) exceed D , then spatial extension of the recorded interference pattern is limited to the domain of existence of the Fourier transform of the function $t(-x_1, -y_1)$.⁸

Note, that in case of interference pattern localization in the scatterer-imaging plane, the mechanism of its formation is defined by superposition of the two identical speckles of two exposures in the Fourier plane. In its turn, formation of the interference pattern, localized in the hologram plane, is defined by the presence of a slope angle of the subjective speckle-field, corresponding to the second exposure, with respect to those of the first exposure, in this plane.

To analyze the behavior dynamics of the fringes, localized in the scatterer-imaging plane, consider the procedure of spatial filtration of the diffraction field in the hologram plane in Fig. 2 exterior to the optical axis, i.e., when the filtering aperture is centered at $(x_{04}, 0)$. Assume that the size of the subjective speckle in the hologram plane is much less than the diameter of filtering aperture, but the angle of slope of the

subjective speckle, caused by diffraction of a plane wave, propagating at the angle $x_{04}/\mu l$ with respect to the optical axis, is constant within the filtering aperture diameter. Then, with accounting for the above condition ($[kax_4/\mu l] \leq \pi$), define the distribution of the field complex amplitude at the spatial filter outlet as

$$u(x_4, y_4) \sim p_0(x_4, y_4) \left\{ F(x_4 + x_{04}, y_4) \otimes \right. \\ \otimes \exp \left\{ -\frac{ikR}{2l(R + \mu^2 l)} [(x_4 + x_{04})^2 + y_4^2] \right\} \otimes \\ \otimes \exp \left(-\frac{ikx_{04}x_4}{\mu l} \right) P_1(x_4, y_4) \otimes \exp \left(-\frac{ikx_{04}x_4}{\mu l} \right) \times \\ \times P_2(x_4, y_4) + \exp \left[-\frac{ik(R + \mu^2 l)}{2\mu^2 Rl} a^2 \right] F(x_4 + x_{04}, y_{04}) \otimes \\ \otimes \exp \left\{ -\frac{ikR}{2l(R + \mu^2 l)} [(x_4 + x_{04})^2 + y_4^2] \right\} \otimes \\ \otimes \exp \left(-\frac{ikax_{04}}{\mu l} \right) \exp \left(-\frac{ikax_{04}x_4}{\mu l} \right) \times \\ \times P_1 \left(x_4 + \frac{R + \mu^2 l}{\mu R} a, y_4 \right) \otimes \exp \left(-\frac{ikx_{04}x_4}{\mu l} \right) P_2(x_4, y_4) \left. \right\}. \quad (18)$$

As a result of the Fourier transform, this distribution in the far focal plane (x_5, y_5) of the lens L'_0 (see Fig. 2) takes the form

$$u(x_5, y_5) \sim \left\{ p_1 \left(\frac{\Delta + \mu l_2}{f_0} x_5 + \frac{\Delta + \mu l_2}{\mu l} x_{04}, \frac{\Delta + \mu l_2}{f_0} y_5 \right) \times \right. \\ \times p_2 \left(\frac{l_2}{f_0} x_5 + \frac{l_2}{\mu l} x_{04}, \frac{l_2}{f_0} y_5 \right) + \\ + p_1 \left(\frac{\Delta + \mu l_2}{f_0} x_5 + \frac{\Delta + \mu l_2}{\mu l} (x_{04} + a), \frac{\Delta + \mu l_2}{f_0} y_5 \right) \times \\ \times p_2 \left(\frac{l_2}{f_0} x_5 + \frac{l_2}{\mu l} (x_{04} + a), \frac{l_2}{f_0} y_5 \right) \exp \left[\frac{ik(R + \mu^2 l)}{2\mu^2 Rl} a^2 \right] \times \\ \times \exp \left[\frac{ik(R + \mu^2 l)}{\mu R f_0} ax_5 - \frac{k}{\mu l} ax_{04} + \frac{k(R + \mu^2 l)}{\mu^2 Rl} ax_{04} \right] \times \\ \times t \left(-\frac{\mu l}{f_0} x_5, -\frac{\mu l}{f_0} y_5 \right) \exp \left[\frac{ikl(R + \mu^2 l)}{2Rf_0^2} (x_5^2 + y_5^2) \right] \times \\ \left. \times \exp \left(\frac{i2kx_{04}x_5}{f_0} \right) \otimes P_0(x_5, y_5) \right\}. \quad (19)$$

Then, with accounting for smallness of $(\Delta + \mu l_2)a/\mu l$ and $l_2 a/\mu l$ in comparison with $(\Delta + \mu l_2)x_{04}/\mu l$ and $l_2 x_{04}/\mu l$, the light distribution in recording plane 3 (see Fig. 2) is defined by the equation

$$\begin{aligned}
 I(x_5, y_5) \sim & \left\{ 1 + \cos \left[\frac{k(R + \mu^2 l) a^2}{2\mu^2 R l} + \frac{k(R + \mu^2 l)}{\mu R f_0} a x_5 - \right. \right. \\
 & \left. \left. - \frac{k}{\mu l} a x_{04} + \frac{k(R + \mu^2 l)}{\mu^2 R l} a x_{04} \right] \right\} \times \\
 & \times \left| p_1 \left(\frac{\Delta + \mu l_2}{f_0} x_5 + \frac{\Delta + \mu l_2}{\mu l} x_{04}, \frac{\Delta + \mu l_2}{f_0} y_5 \right) \times \right. \\
 & \times p_2 \left(\frac{l_2}{f_0} x_5 + \frac{l_2}{\mu l} x_{04}, \frac{l_2}{f_0} y_5 \right) t \left(-\frac{\mu l}{f_0} x_5, -\frac{\mu l}{f_0} y_5 \right) \times \\
 & \times \exp \left[\frac{i k l (R + \mu^2 l)}{2 R f_0^2} (x_5^2 + y_5^2) \right] \times \\
 & \left. \times \exp \left(\frac{i 2 k x_{04} x_5}{f_0} \right) \otimes P_0(x_5, y_5) \right|^2. \quad (20)
 \end{aligned}$$

It follows from Eq. (20) that when the filtering aperture is displaced on the x -axis with accounting for the above inequality, i.e., $l_2 < (\Delta + \mu l_2)/\mu$, the Galilean telescope pupil is displaced relative to static image of the scatterer; in addition, fringes are also displaced. In this case, while varying x_{04} , the interference pattern phase changes by π when displacing the filtering aperture center, e.g., from a minimum of interference pattern, localized in the hologram plane, to its maximum ("living" fringes).

When spatial filtration of the diffraction field is carried out in the scatterer-imaging plane exterior to the optical axis, e.g., at the point $(x_{05}, 0)$, at retrieving the double-exposure quasi-Fourier hologram, and the phase change $[k(R + \mu^2 l) a x_5 / \mu R l] \leq \pi$ within the diameter of filtering aperture, the distribution of the field complex amplitude takes the form

$$\begin{aligned}
 u(x_5, y_5) \sim & p_0(x_5, y_5) \left\{ \exp \left\{ \frac{i k l (R + \mu^2 l)}{2 R f_0^2} [(x_5 + x_{05})^2 + y_5^2] \right\} \otimes \right. \\
 & \otimes F_1(x_5 + x_{05}, y_5) \exp \left\{ -\frac{i k l (R + \mu^2 l)}{2 R f_0^2} [(x_5 + x_{05})^2 + y_5^2] \right\} + \\
 & + \exp \left[\frac{i k (R + \mu^2 l)}{2 \mu^2 R l} a^2 \right] \exp \left[\frac{i k (R + \mu^2 l)}{\mu R f_0} a x_{05} \right] \times \\
 & \times \exp \left\{ \frac{i k l (R + \mu^2 l)}{2 R f_0^2} \left[\left(x_5 + x_{05} - \frac{f_0}{\mu l} a \right)^2 + y_5^2 \right] \right\} \otimes \\
 & \left. \otimes F_1(x_5 + x_{05}, y_5) \exp \left\{ -\frac{i k l (R + \mu^2 l)}{2 R f_0^2} [(x_5 + x_{05})^2 + y_5^2] \right\} \right\}. \quad (21)
 \end{aligned}$$

After fulfillment of the Fourier transform, the field complex amplitude distribution in the far focal plane of the lens L'_0 (see Fig. 3) is defined as

$$\begin{aligned}
 u(x_6, y_6) \sim & \left\{ 1 + \exp \left[\frac{i k (R + \mu^2 l)}{2 \mu^2 R l} a^2 \right] \times \right. \\
 & \times \exp \left[\frac{i k (R + \mu^2 l)}{\mu R f_0} a x_{05} \right] \exp \left(-\frac{i k a x_6}{\mu l} \right) \left. \right\} \exp \left(\frac{i 2 k x_{05} x_6}{f_0} \right) \times \\
 & \times \exp \left[-\frac{i k R}{2 l (R + \mu^2 l)} (x_6^2 + y_6^2) \right] \left\{ t \left(-\frac{\mu R}{R + \mu^2 l} x_6, -\frac{\mu R}{R + \mu^2 l} y_6 \right) \otimes \right. \\
 & \left. \otimes \exp \left[\frac{i k R}{2 l (R + \mu^2 l)} (x_6^2 + y_6^2) \right] \right\} \otimes P_0(x_6, y_6). \quad (22)
 \end{aligned}$$

Based on Eq. (22) and with accounting for the integral convolution representation, the light distribution in recording plane 3 (see Fig. 3) takes the form

$$\begin{aligned}
 I(x_6, y_6) \sim & \\
 \sim & \left\{ 1 + \cos \left[\frac{k(R + \mu^2 l)}{2\mu^2 R l} a^2 - \frac{k a x_6}{\mu l} + \frac{k(R + \mu^2 l)}{\mu R f_0} a x_{05} \right] \right\} \times \\
 & \times \left\{ F(-x_6, -y_6) \otimes \exp \left[-\frac{i k R}{2 l (R + \mu^2 l)} (x_6^2 + y_6^2) \right] \right\} \times \\
 & \times \exp \left(\frac{i 2 k x_{05} x_6}{f_0} \right) \otimes P_0(x_6, y_6) \Big|^2. \quad (23)
 \end{aligned}$$

As follows from Eq. (23), when the filtering aperture is displaced along the x -axis, the interference pattern displaces relative to a fixed image. Besides, while varying x_{05} , the interference pattern phase changes by π when displacing the filtering aperture center, e.g., from a minimum of interference pattern, localized in the scatterer-imaging plane, to its maximum ("living" fringes). In addition, in case of the two-exposure recording of the Fourier hologram, "frozen" fringes are formed in their plane while reconstructing due to the absence of displacements of the subjective speckles, corresponding to the second exposure.

A comparison of the considered holographic interferometer, used for controlling transversal displacement of the scatterer, with those using the Kepler tube¹ shows that interference patterns are also localized in two planes, i.e., the hologram and Fourier ones. The behavior dynamics of fringes is similar when recording the interference patterns with spatial filtering of the diffraction field in the corresponding planes of their localization exterior the optical axis. However, in the interferometer, using the Galilean telescope, the interference pattern, localized in the scatterer-imaging plane, is formed in the Fourier plane and characterized by a nonlinear dependence of interferometer sensitivity on the telescope magnification at $R \neq \infty$, as well as on the sign of curvature of a spherical wave of the coherent

radiation used to illuminate the scatterer. In its turn, the interferometer sensitivity to the interference pattern, localized in the hologram plane, depends on the hologram-plane scale of the Fourier transform of the function, characterizing the complex amplitude of scatterer transmittance or reflection, in this plane.

In the experiment, double-exposure holograms were recorded on Mikrat VRL photoplates by means of 0.6328 μm He–Ne laser radiation. The experimental technique consisted in comparison of the hologram records made with a Galilean telescope with the following parameters: $f_1 = 250$ mm, $f_2 = 120$ mm, $d_1 = 31$ mm, $d_2 = 15$ mm. For the fixed values of transversal scatterer: the displacement $a = (0.025 \pm 0.002)$ mm, distances $l_1 = 200$ mm and $l_2 = 150$ mm, curvature of a divergent spherical spatially restricted reference beam $r = 258.5$ mm with the angle $\theta = 12^\circ$, different curvatures of spherical waves front of the coherent radiation, used for opaque screen illumination, were chosen within a range $300 \text{ mm} \leq |R| \leq \infty$; a diameter of illuminated area was 40 mm.

Figure 4 shows the interference patterns, localized in the Fourier plane, where the opaque screen is imaged, and the characterizing transversal displacement of the screen. The interference patterns were recorded in the lens focal plane with $f_2 = 135$ mm when spatial filtering the diffraction field in the hologram plane by means of its reconstruction with a small-aperture (≈ 2 mm) laser beam.

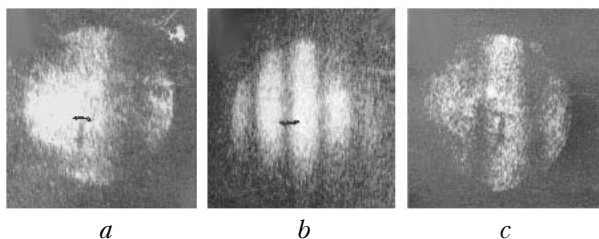


Fig. 4. Interference patterns localized in the plane of scatterer imaging and characterizing its transversal displacement: the scatterer is illuminated by a collimated beam (a), radiation with divergent (b) and convergent (c) spherical waves.

When recording the hologram, the scatterer was illuminated by a collimated beam (Fig. 4a), the coherent radiation with convergent ($R = 500$ mm, Fig. 4b) and divergent ($R = 400$ mm, Fig. 4c) spherical waves. The letter “T” was preliminary drawn on the opaque screen. In this case, the spatial extension s of interference patterns in the focal plane of the lens L'_0 was 9.6 mm, which agrees with the calculated value.

The interference pattern, localized in the hologram plane, is shown in Fig. 5a. It was recorded at illuminating the hologram (see Fig. 3) by a collimated beam of 50 mm in diameter; spatial filtration of the diffraction field was carried out in the focal plane of the lens L_0 of 60 mm in diameter and 500 mm in focal length. In this case, spatial extension of the interference pattern was 43 mm and corresponded to

the calculated value D with accounting for a factor of 1.22. In addition, there was no need in spatial filtration of the diffraction field in the frequency plane of two-component optical system in Fig. 3 in case of the Fourier hologram recording.

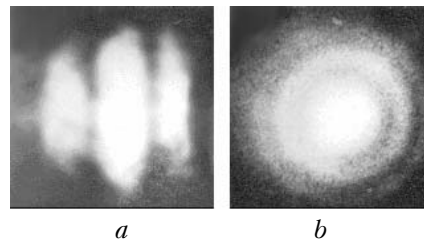


Fig. 5. Interference patterns localized in the hologram plane and characterizing transversal (a) and longitudinal (b) displacement of the scatterer.

The periods of the fringes, localized both in the Fourier and hologram planes, were calculated for the known variables $\lambda, a, \mu, l, R,$ and f_0 and compared with measurement results. They agreed to each other up to 10% error, allowable in the experiment.

Let opaque screen 1 be z -axial displaced to $\Delta l \ll l_1, R$ before the second exposure of photoplate 2 (see Fig. 1). Then define the distribution of the field complex amplitude, corresponding to the second exposure, in the object channel in the photoplate plane (to the used approximation) as

$$\begin{aligned}
 u'_2(x_4, y_4) \sim & \exp(ik\Delta l) \iiint \iiint \int_{-\infty}^{\infty} t(x_1, y_1) \times \\
 & \times \exp\left[\frac{ik}{2(R - \Delta l)}(x_1^2 + y_1^2)\right] \times \\
 & \times \exp\left\{\frac{ik}{2(l_1 + \Delta l)}[(x_1 - x_2)^2 + (y_1 - y_2)^2]\right\} p_1(x_2, y_2) \times \\
 & \times \exp\left[-\frac{ik}{2f_1}(x_2^2 + y_2^2)\right] \exp\left\{\frac{ik}{2\Delta}[(x_2 - x_3)^2 + (y_2 - y_3)^2]\right\} \times \\
 & \times p_2(x_3, y_3) \exp\left[\frac{ik}{2f_2}(x_3^2 + y_3^2)\right] \times \\
 & \times \exp\left\{\frac{ik}{2l_2}[(x_3 - x_4)^2 + (y_3 - y_4)^2]\right\} dx_1 dy_1 dx_2 dy_2 dx_3 dy_3,
 \end{aligned} \tag{24}$$

which while fulfilling the transforms, known in the Fourier optics, takes the following form:

$$\begin{aligned}
 u_2(x_4, y_4) \sim & \exp(ik\Delta l) \exp\left[\frac{ik}{2l_2}(x_4^2 + y_4^2)\right] \times \\
 & \times \left\{ \exp\left[-\frac{ikL_1}{2l_2^2}(x_4^2 + y_4^2)\right] \right\} \left\{ \exp\left[-\frac{ikL'_1 L'_2}{2l_2^2 \Delta^2}(x_4^2 + y_4^2)\right] \right\} \times \\
 & \times \int \int_{-\infty}^{\infty} t(x_1, y_1) \exp\left[\frac{ik(R + l_1)}{2(R - \Delta l)(l_1 + \Delta l)}(x_1^2 + y_1^2)\right] \times
 \end{aligned}$$

$$\begin{aligned} &\times \exp\left[-\frac{ikL'_2}{(l_1 + \Delta l)^2}(x_1^2 + y_1^2)\right] \exp\left[-\frac{ikL_1L'_2}{(l_1 + \Delta l)l_2\Delta}(x_1x_4 + y_1y_4)\right] \times \\ &\times dx_1dy_1 \otimes P_1(x_4, y_4) \Big\} \otimes P_2(x_4, y_4) \Big\}, \end{aligned} \quad (25)$$

where $(1/L'_2) = 1/(l_1 + \Delta l) - 1/f_1 + 1/\Delta - L_1/\Delta^2$ is the notation, introduced for brevity.

Since $L_1 = l_2\Delta/(\Delta + \mu l_2)$ and $L'_2 = (l_1 + \Delta l)(\Delta + \mu l_2)/\mu(l_1 + \Delta l/\mu^2)$, then after calculating Eq. (25) with accounting for the conditions used in derivation of Eq. (4), the distribution of the field complex amplitude $u'_2(x_4, y_4)$ within the above area in the plane of a photoplate of D in diameter takes the form

$$\begin{aligned} u'_2(x_4, y_4) &\sim \exp(ik\Delta l) \exp\left[\frac{ik}{2r}(x_4^2 + y_4^2)\right] \times \\ &\times \exp\left[-\frac{ik\Delta l}{2\mu^2l^2}(x_4^2 + y_4^2)\right] \Big\{ F'(x_4, y_4) \otimes \\ &\otimes \exp\left[-\frac{ik(R - \Delta l)(\mu^2l + \Delta l)}{2(R + \mu^2l)\mu^2l^2}(x_4^2 + y_4^2)\right] \otimes \\ &\otimes P_1(x_4, y_4) \otimes P_2(x_4, y_4) \Big\}, \end{aligned} \quad (26)$$

where $F'(x_4, y_4)$ is the Fourier transform of $t(x_1, y_1)$ with the spatial frequencies $x_4/\lambda\mu l (1 + \Delta l/\mu^2l)$ and $y_4/\lambda\mu l (1 + \Delta l/\mu^2l)$.

If the quasi-Fourier or Fourier hologram is double-exposure recording with a divergent spherical reference wave with the curvature $r = l$ on the linear part of the photomaterial blackening curve, the distribution of the complex amplitude of the hologram transmittance, corresponding to the (-1) -st diffraction order, on the base of Eqs. (4) and (26) takes the form

$$\begin{aligned} \tau'(x_4, y_4) &\sim \exp(-ikx_4 \sin\theta) \Big\{ F(x_4, y_4) \otimes \\ &\otimes \exp\left[-\frac{ikR}{2l(R + \mu^2l)}(x_4^2 + y_4^2)\right] \otimes P_1(x_4, y_4) \otimes P_2(x_4, y_4) + \\ &+ \exp(ik\Delta l) \exp\left[-\frac{ik\Delta l}{2\mu^2l^2}(x_4^2 + y_4^2)\right] \Big\{ F'(x_4, y_4) \otimes \\ &\otimes \exp\left[-\frac{ik(R - \Delta l)(\mu^2l + \Delta l)}{2(R + \mu^2l)\mu^2l^2}(x_4^2 + y_4^2)\right] \otimes \\ &\otimes P_1(x_4, y_4) \otimes P_2(x_4, y_4) \Big\}. \end{aligned} \quad (27)$$

It follows from Eq. (27) that an inhomogeneous (radially varying from the optical axis) displacement of the subjective speckles, corresponding to the second exposure, with respect to the similar¹⁰ speckles of the first exposure takes place in the hologram plane due to the difference in the scales of Fourier transforms $F(x_4, y_4)$ and $F'(x_4, y_4)$. This displacement is independent of the curvature R of a spherical wave of the coherent radiation used for scatterer illumination while recording the hologram. At the same time, the

exponential factor $\exp\left[\frac{-ik\Delta l(x_4^2 + y_4^2)}{2\mu^2l^2}\right]$ indicates the

presence of a slope, radially varying from the optical axis, of subjective speckles, corresponding to the second exposure; the slope is also R -independent. The orientation character of the subjective speckles, corresponding to the second exposure, is so that there is an additional radial variation of the slope from the optical axes, which is caused in Eq. (27) by

the factor $\exp\left[-\frac{ik(R - \Delta l)(\mu^2l + \Delta l)}{2(R + \mu^2l)\mu^2l^2}(x_4^2 + y_4^2)\right]$ under

the convolution integral. This variation depends on the curvature of a spherical wave of the coherent radiation used for scatterer illumination.

Let spatial filtration of the diffraction field be carried out in the hologram plane on the optical axis when reconstructing the double-exposure hologram, characterizing longitudinal displacement of the scatterer (Fig. 2). Let also the Fourier transforms $F(x_4, y_4)$ and $F'(x_4, y_4)$ of the function $t(x_1, y_1)$ be similar within the diameter d_f of the filtering aperture, which is in this case to satisfy the condition $d_f \leq \lambda\mu^2l(\Delta + \mu l_2)/d_1\Delta l$. Besides, if the phase change $k\Delta l(x_4^2 + y_4^2)/2\mu^2l^2$ does not exceed π within the diameter of the filtering aperture, then the distribution of the field complex aperture at the outlet of the spatial filter p_0 (see Fig. 2) takes the form

$$\begin{aligned} u'(x_4, y_4) &\sim p_0(x_4, y_4) \Big\{ F(x_4, y_4) \otimes \\ &\otimes \exp\left[-\frac{ikR}{2l(R + \mu^2l)}(x_4^2 + y_4^2)\right] \otimes P_1(x_4, y_4) \otimes P_2(x_4, y_4) + \\ &+ \exp(ik\Delta l) \Big\{ F(x_4, y_4) \otimes \\ &\otimes \exp\left[-\frac{ik(R - \Delta l)(\mu^2l + \Delta l)}{2(R + \mu^2l)\mu^2l^2}(x_4^2 + y_4^2)\right] \otimes \\ &\otimes P_1(x_4, y_4) \otimes P_2(x_4, y_4) \Big\}. \end{aligned} \quad (28)$$

Based on Eq. (28), the distribution of the field complex aperture in recording plane 3 (see Fig. 2) after the Fourier transform is defined by the equation

$$u'(x_5, y_5) \sim \left\{ \left[1 + \exp(ik\Delta l) \exp \left[\frac{ik(R^2 - \mu^4 l^2) \Delta l}{2\mu^2 R^2 f_0^2} (x_5^2 + y_5^2) \right] \right] \times \right. \\ \times p_1 \left(\frac{\Delta + \mu l_2}{f_0} x_5, \frac{\Delta + \mu l_2}{f_0} y_5 \right) \times \\ \times p_2 \left(\frac{l_2}{f_0} x_5, \frac{l_2}{f_0} y_5 \right) t \left(-\frac{\mu l}{f_0} x_5, -\frac{\mu l}{f_0} y_5 \right) \times \\ \left. \times \exp \left[\frac{ikl(R + \mu^2 l)}{2Rf_0^2} (x_5^2 + y_5^2) \right] \right\} \otimes P_0(x_5, y_5). \quad (29)$$

If the variation period of $1 + \exp(ik\Delta l) \times \exp \left[\frac{ik(R^2 - \mu^4 l^2) \Delta l}{2\mu^2 R^2 f_0^2} (x_5^2 + y_5^2) \right]$ is at least one order of magnitude larger than the width of the function $P_0(x_5, y_5)$, then take it out of the convolution integral in Eq. (29), and the light distribution in the plane (x_5, y_5) with accounting for the inequality $l_2 < (\Delta + \mu l_2)/\mu$ takes the form

$$I'(x_5, y_5) \sim \left\{ 1 + \cos \left[k\Delta l + \frac{k(R^2 - \mu^4 l^2) \Delta l}{2\mu^2 R^2 f_0^2} (x_5^2 + y_5^2) \right] \right\} \times \\ \times \left| p_1 \left(\frac{\Delta + \mu l_2}{f_0} x_5, \frac{\Delta + \mu l_2}{f_0} y_5 \right) t \left(-\frac{\mu l}{f_0} x_5, -\frac{\mu l}{f_0} y_5 \right) \times \right. \\ \left. \times \exp \left[\frac{ikl(R + \mu^2 l)}{2Rf_0^2} (x_5^2 + y_5^2) \right] \otimes P_0(x_5, y_5) \right|^2. \quad (30)$$

According to Eq. (30), a subjective speckle structure in the plane of scatterer imaging, restricted to the image of Galilean telescope pupil, is modulated by fringes of equal slope – the system of concentric interference rings. The measurement of their radii r_1 and r_2 in the neighboring interference orders allows determination of the longitudinal scatterer displacement $\Delta l = 2\lambda\mu^2 R^2 f_0^2 / (R^2 - \mu^4 l^2)(r_2^2 - r_1^2)$ for the known variables λ , μ , R , l , and f_0 . The interferometer sensitivity in this case depends on the curvature of the spherical wave front of the coherent radiation, used for scatterer illumination while recording the hologram. Thus, when $|R|$ decreases within a range $\mu^2 l \leq |R| \leq \infty$, the interferometer sensitivity decreases down to zero when $|R| = \mu^2 l$. In this case, an additional slope of subjective speckles, corresponding to the second exposure, with respect to the similar ones of the first exposure in the hologram plane is radially invariable from the optical axis in Eq. (26). A further decrease of the spherical wave curvature results in enhancement of the interferometer sensitivity when recording the interference pattern, localized in the scatterer-imaging plane, due to occurrence and an increase of a slope, radially varied from the optical axis, of the subjective speckles, corresponding to the second exposure, in the hologram plane.

Consider the spatial filtration of the diffraction field on the optical axis in the scatterer-imaging plane (x_5, y_5) (Fig. 3) at the stage of recording of the double-exposure quasi-Fourier hologram, characterizing longitudinal scatterer displacement. In this case, neglecting the spatial boundedness of the field due to finite sizes of the hologram and the lens L'_0 , the distribution of its complex amplitude in the above plane is defined as

$$u'(x_5, y_5) \sim p_1 \left(\frac{\Delta + \mu l_2}{f_0} x_5, \frac{\Delta + \mu l_2}{f_0} y_5 \right) p_2 \left(\frac{l_2}{f_0} x_5, \frac{l_2}{f_0} y_5 \right) \times \\ \times t \left(-\frac{\mu l}{f_0} x_5, -\frac{\mu l}{f_0} y_5 \right) \exp \left[\frac{ikl(R + \mu^2 l)}{2Rf_0^2} (x_5^2 + y_5^2) \right] + \\ + \exp(ik\Delta l) \exp \left[\frac{ik\mu^2 l^2}{2f_0^2 \Delta l} (x_5^2 + y_5^2) \right] \otimes \\ \otimes \left\{ p_1 \left(\frac{\Delta + \mu l_2}{f_0} x_5, \frac{\Delta + \mu l_2}{f_0} y_5 \right) p_2 \left(\frac{l_2}{f_0} x_5, \frac{l_2}{f_0} y_5 \right) \times \right. \\ \times t \left[-\frac{\mu l}{f_0} \left(1 + \frac{\Delta l}{\mu^2 l} \right) x_5, -\frac{\mu l}{f_0} \left(1 + \frac{\Delta l}{\mu^2 l} \right) y_5 \right] \times \\ \times \exp \left[\frac{ik(R^2 - \mu^4 l^2) \Delta l}{2\mu^2 R^2 f_0^2} (x_5^2 + y_5^2) \right] \times \\ \left. \times \exp \left[\frac{ikl(R + \mu^2 l) \Delta l}{2Rf_0^2} (x_5^2 + y_5^2) \right] \right\}. \quad (31)$$

Knowing that $\exp \left[ik\mu^2 l^2 (x_5^2 + y_5^2) / 2f_0^2 \Delta l \right] \cong \delta(x_5, y_5)$ set the phase change $\left[k(R^2 - \mu^4 l^2) \times \Delta l (x_5^2 + y_5^2) / 2\mu^2 R^2 f_0^2 \right] \leq \pi$ within the diameter of the filtering aperture of the spatial filter p_0 (Fig. 3). Besides, $d_t \leq \lambda\mu^2 l(\Delta + \mu l_2) / d_l \Delta l$, if $f_0 = \mu l$; when $f_0 \neq \mu l$, it is necessary to take into account the factor $f_0/\mu l$. Hence, the distribution of the field complex amplitude at the spatial filter outlet takes the form

$$u'(x_5, y_5) \sim p_0(x_5, y_5) \left\{ t \left(-\frac{\mu l}{f_0} x_5, -\frac{\mu l}{f_0} y_5 \right) \times \right. \\ \times \exp \left[\frac{ikl(R + \mu^2 l)}{2Rf_0^2} (x_5^2 + y_5^2) \right] + \exp(ik\Delta l) \times \\ \times \exp \left[\frac{ik\mu^2 l^2}{2f_0^2 \Delta l} (x_5^2 + y_5^2) \right] \otimes t \left(-\frac{\mu l}{f_0} x_5, -\frac{\mu l}{f_0} y_5 \right) \times \\ \left. \times \exp \left[\frac{ikl(R + \mu^2 l)}{2Rf_0^2} (x_5^2 + y_5^2) \right] \right\}. \quad (32)$$

On the base of Eq. (32) after fulfillment of the Fourier transform, the distribution of the field complex amplitude in the plane (x_6, y_6) (Fig. 3) is defined as

$$u'(x_6, y_6) \sim \left\{ 1 + \exp(ik\Delta l) \exp\left[-\frac{ik\Delta l}{2\mu^2 l^2}(x_6^2 + y_6^2)\right] \right\} \times \left\{ F(-x_6, -y_6) \otimes \exp\left[-\frac{ikR}{2l(R + \mu^2 l)}(x_6^2 + y_6^2)\right] \right\} \otimes P_0(x_6, y_6). \tag{33}$$

If the variation period of $1 + \exp(ik\Delta l) \times \exp\left[-\frac{ik\Delta l}{2\mu^2 l^2}(x_6^2 + y_6^2)\right]$ is at least one order of magnitude larger than the width of $P_0(x_6, y_6)$, defining the size of subjective speckle in recording plane 3 (Fig. 3), then we take it out of the convolution integral in Eq. (33), and the light distribution in the plane (x_6, y_6) takes the form

$$I'(x_6, y_6) \sim \left\{ 1 + \cos\left[k\Delta l - \frac{k\Delta l}{2\mu^2 l^2}(x_6^2 + y_6^2)\right] \right\} \times \left\{ F(-x_6, -y_6) \otimes \exp\left[-\frac{ikR}{2l(R + \mu^2 l)}(x_6^2 + y_6^2)\right] \right\} \otimes P_0(x_6, y_6)^2. \tag{34}$$

According to Eq. (33), a subjective speckle structure in the hologram plane is modulated by fringes of equal slope – the system of concentric interference rings. Measurement of their radii in the neighboring interference orders allows determination of the longitudinal scatterer displacement for the known variables λ , μ , and l . In this case, the interferometer sensitivity depends on the scale of Fourier-transform function, characterizing the complex amplitude of scatterer transmittance or reflection, in the plane of photoplate 2 (see Fig. 1). Besides, if diameters of a collimated beam of the coherent radiation, reconstructing the hologram, and of the lens L'_0 (Fig. 3), exceed D , the spatial extension of the recorded interference pattern is limited to the domain of existence of the Fourier transform of $t(-x_1, -y_1)$ in the hologram plane.

Note, that in case of localization of the interference pattern, characterizing longitudinal scatterer displacement, in the hologram plane, the mechanism of its formation is caused by the presence of a slope angle of the subjective speckle-field, corresponding to the second exposure, with respect to the field of the first exposure in the hologram plane. The angle varies radially from the optical axis and is independent of the curvature of a spherical wave of the coherent radiation, used for scatterer illumination. In its turn, the orientation character of the subjective speckles, corresponding to the second exposure and correlated with variations of the slope angle, depending on the curvature of a spherical wave of the coherent radiation, used for scatterer illumination, governs the

localization of the interference pattern in the scatterer-imaging plane.

To analyze the behavior dynamics of the fringes, localized in the scatterer-imaging plane and characterizing longitudinal displacement of the scatterer, consider spatial filtration of the diffraction field in the hologram plane exterior the optical axis (Fig. 2), i.e., the case when the filtering aperture is centered at $(x_{04}, 0)$. As in the case of transversal scatterer displacement, assume that the size of a subjective speckle in the hologram plane is much less than the filtering aperture diameter, but within the latter, the angle of slope of the subjective speckle, caused by the diffraction of a plane wave, propagating at the $x_{04}/\mu l$ angle to the optical axis, is invariable. In addition, the phase change $[k\Delta l(x_4^2 + y_4^2)/2\mu^2 l^2] \leq \pi$ within the filtering aperture diameter $d_f \leq \lambda\mu^2 l(\Delta + \mu l_2)/d_1 \Delta l$. Then define the distribution of the field complex amplitude at the spatial filter outlet as

$$u'(x_4, y_4) \sim p_0(x_4, y_4) \left\{ F(x_4 + x_{04}, y_4) \otimes \exp\left[-\frac{ikR}{2l(R + \mu^2 l)}[(x_4 + x_{04})^2 + y_4^2]\right] \right\} \otimes \exp\left(-\frac{ikx_{04}x_4}{\mu l}\right) P_1(x_4, y_4) \otimes \exp\left(-\frac{ikx_{04}x_4}{\mu l}\right) P_2(x_4, y_4) + \exp(ik\Delta l) \exp\left(-\frac{ik\Delta l x_{04}^2}{2\mu^2 l^2}\right) \times \left\{ \int_{-\infty}^{\infty} \int_{-\infty}^{\infty} t(x_1, y_1) \exp\left(\frac{ik\Delta l x_1 x_{04}}{\mu^3 l^2}\right) \times \exp\left[-\frac{ik[x_1(x_4 + x_{04}) + y_1 y_4]}{\mu l}\right] dx_1 dy_1 \otimes \exp\left[-\frac{ik(R - \Delta l)(\mu^2 l + \Delta l)}{2(R + \mu^2 l)\mu^2 l^2}[(x_4 + x_{04})^2 + y_4^2]\right] \otimes \exp\left(-\frac{ikx_{04}x_4}{\mu l}\right) P_1(x_4, y_4) \otimes \exp\left(-\frac{ikx_{04}x_4}{\mu l}\right) P_2(x_4, y_4) \right\}. \tag{35}$$

After fulfillment of the Fourier transform, the distribution of the field complex amplitude in the far focal plane L'_0 (see Fig. 2) takes the form

$$u'(x_5, y_5) \sim \left\{ 1 + \exp(ik\Delta l) \exp\left(-\frac{ik\Delta l x_{04}^2}{2\mu^2 l^2}\right) \times \exp\left(-\frac{ik\Delta l}{\mu^2 l f_0} x_{04} x_5\right) \exp\left[\frac{ik(R^2 - \mu^4 l^2)\Delta l}{2\mu^2 R^2 f_0^2}(x_5^2 + y_5^2)\right] \right\} \times p_1\left(\frac{\Delta + \mu l_2}{f_0} x_5 + \frac{\Delta + \mu l_2}{\mu l} x_{04}, \frac{\Delta + \mu l_2}{f_0} y_5\right) \times$$

$$\begin{aligned} & \times p_2 \left(\frac{l_2}{f_0} x_5 + \frac{l_2}{\mu l} x_{04}, \frac{l_2}{f_0} y_5 \right) t \left(-\frac{\mu l}{f_0} x_5, -\frac{\mu l}{f_0} y_5 \right) \times \\ & \times \exp \left[\frac{ikl(R + \mu^2 l)}{2Rf_0^2} (x_5^2 + y_5^2) \right] \exp \left(\frac{i2kx_{04}x_5}{f_0} \right) \otimes P_0(x_5, y_5). \end{aligned} \quad (36)$$

On the base of Eq. (36) and with accounting for the inequality $l_2 < (\Delta + \mu l_2)/\mu$, define the light distribution in recording plane 3 (see Fig. 2) as

$$\begin{aligned} I'(x_5, y_5) \sim & \left\{ 1 + \cos \left[k\Delta l + \frac{k(R^2 - \mu^4 l^2)\Delta l}{2\mu^2 R^2 f_0^2} (x_5^2 + y_5^2) - \right. \right. \\ & \left. \left. - \frac{k\Delta l}{\mu^2 l f_0} x_{04} x_5 - \frac{k\Delta l}{2\mu^2 l^2} x_{04}^2 \right] \right\} \times \\ & \times \left| p_1 \left(\frac{\Delta + \mu l_2}{f_0} x_5 + \frac{\Delta + \mu l_2}{\mu l} x_{04}, \frac{\Delta + \mu l_2}{f_0} y_5 \right) \right| \times \\ & \times t \left(-\frac{\mu l}{f_0} x_5, -\frac{\mu l}{f_0} y_5 \right) \exp \left[\frac{ikl(R + \mu^2 l)}{2Rf_0^2} (x_5^2 + y_5^2) \right] \times \\ & \times \exp \left(\frac{i2kx_{04}x_5}{f_0} \right) \otimes P_0(x_5, y_5) \Big|^2. \end{aligned} \quad (37)$$

As follows from Eq. (37), when the filtering aperture is displaced on the x -axis, an image of the Galilean telescope pupil displaces in respect to a relatively immovable scatterer image. Fringes also displace due to an inhomogeneous displacement of the subjective speckles, corresponding to the second exposure, in the hologram plane (fringe parallax). In this case, while varying x_{04} , the interference pattern phase changes when displacing the filtering aperture center, e.g., from a minimum of interference pattern, localized in the hologram plane, to its maximum ("living" fringes).

When spatial filtration of the diffraction field is carried out in the scatterer-imaging plane exterior the optical axis in Fig. 3, e.g., at the point $(x_{05}, 0)$, while reconstructing the double-exposure quasi-Fourier hologram, and the phase change $\left[k(R^2 - \mu^4 l^2)\Delta l(x_5^2 + y_5^2)/2\mu^2 R^2 f_0^2 \right] \leq \pi$ within the diameter of filtering aperture, the distribution of the field complex amplitude at the spatial filter outlet is defined as

$$\begin{aligned} u'(x_5, y_5) \sim & p_0(x_5, y_5) \left\{ t \left[-\frac{\mu l}{f_0} (x_5 + x_{05}), -\frac{\mu l}{f_0} y_5 \right] \times \right. \\ & \times \exp \left\{ \frac{ikl(R + \mu^2 l)}{2Rf_0^2} [(x_5 + x_{05})^2 + y_5^2] \right\} + \exp(ik\Delta l) \times \\ & \times \exp \left[\frac{ik(R^2 - \mu^4 l^2)\Delta l x_{05}^2}{2\mu^2 R^2 f_0^2} \right] \exp \left[\frac{ik\mu^2 l^2}{2f_0^2 \Delta l} (x_5^2 + y_5^2) \right] \otimes \end{aligned}$$

$$\begin{aligned} & \otimes t \left[-\frac{\mu l}{f_0} \left(1 + \frac{\Delta l}{\mu^2 l} \right) (x_5 + x_{05}), -\frac{\mu l}{f_0} \left(1 + \frac{\Delta l}{\mu^2 l} \right) y_5 \right] \times \\ & \times \exp \left\{ \frac{ikl(R + \mu^2 l)}{2Rf_0^2} [(x_5 + x_{05})^2 + y_5^2] \right\} \Big\}. \end{aligned} \quad (38)$$

If $d_f \leq \lambda \mu^2 l (\Delta + \mu l_2) / d_1 \Delta l$ ($f_0 = \mu l$), then

$$\begin{aligned} & t \left[-\frac{\mu l}{f_0} \left(1 + \frac{\Delta l}{\mu^2 l} \right) (x_5 + x_{05}), -\frac{\mu l}{f_0} \left(1 + \frac{\Delta l}{\mu^2 l} \right) y_5 \right] = \\ & = t \left[-\frac{\mu l (x_5 + x_{05})}{f_0}, -\frac{\mu l y_5}{f_0} \right] \end{aligned}$$

in Eq. (38) and subjective speckles of two exposures at the spatial filter outlet are identical. Again, the distribution of the field complex amplitude in the far focal plane of the lens L'_0 (see Fig. 3) takes the form

$$\begin{aligned} u'(x_6, y_6) \sim & \left\{ 1 + \exp(ik\Delta l) \exp \left[\frac{ik(R^2 - \mu^4 l^2)\Delta l x_{05}^2}{2\mu^2 R^2 f_0^2} \right] \times \right. \\ & \times \exp \left[-\frac{ik\Delta l}{2\mu^2 l^2} (x_6^2 + y_6^2) \right] \Big\} \exp \left(-\frac{ik\Delta l}{\mu^2 l f_0} x_{05} x_6 \right) \times \\ & \times \left\{ F(-x_6, -y_6) \otimes \exp \left[-\frac{ikR}{2l(R + \mu^2 l)} (x_6^2 + y_6^2) \right] \right\} \otimes \\ & \otimes P_0(x_6, y_6), \end{aligned} \quad (39)$$

on the base of which the light distribution in recording plane 3 (see Fig. 3) is defined as

$$\begin{aligned} I'(x_6, y_6) \sim & \left\{ 1 + \cos \left[k\Delta l - \frac{k\Delta l}{2\mu^2 l^2} (x_6^2 + y_6^2) - \right. \right. \\ & \left. \left. - \frac{k\Delta l}{\mu^2 l f_0} x_{05} x_6 + \frac{k(R^2 - \mu^4 l^2)\Delta l}{2\mu^2 R^2 f_0^2} x_{05}^2 \right] \right\} \times \\ & \times \left| F(-x_6, -y_6) \otimes \exp \left[-\frac{ikR}{2l(R + \mu^2 l)} (x_6^2 + y_6^2) \right] \otimes P_0(x_6, y_6) \right|^2. \end{aligned} \quad (40)$$

According to Eq. (40), when the filtering aperture is displaced along the x -axis, the fringes displace with respect to a relatively immovable hologram image due to an inhomogeneous displacement of the subjective speckles, corresponding to the second exposure, in a direction, depending on the direction of filtering aperture displacement (fringe parallax). In this case, while varying x_{05} , the interference pattern phase changes when displacing the filtering aperture center, e.g., from the minimum of interference pattern, localized in the scatterer-imaging plane, to its maximum ("living" fringes).

When the interference pattern, characterizing longitudinal scatterer displacement, is localized in the Fourier plane, spatial filtration of the diffraction field in the scatterer-imaging plane is required to record this interference pattern. In this case, when displacing the filtering aperture, as in the case of single-component optical system for recording the Fourier hologram,^{11,12} the only fringe parallax takes place due to a similar mechanism of interference pattern formation, connected with accounting for an inhomogeneous displacement of the subjective speckles, corresponding to the second exposure, in the hologram plane.

Comparison of the considered holographic interferometer, used for controlling transversal displacement of the scatterer, with those using the Kepler tube¹ shows that interference patterns are also localized in two planes, i.e., the hologram and Fourier ones. In the interferometer, using the Galilean telescope, the interference pattern, localized in the scatterer-imaging plane, is formed in the Fourier plane; at $R \neq \infty$ it has other character of the sensitivity dependence on the telescope magnification. In its turn, the interferometer sensitivity for the interference pattern, localized in the hologram plane, depends on the hologram-plane scale of the Fourier transform of the function, characterized the complex amplitude of scatterer transmittance or reflection. Besides, when using the Galilean telescope to control longitudinal displacement of the scatterer, the fringe parallax is characteristic when recording the interference patterns with spatial filtration of the diffraction field exterior the optical axis in the corresponding planes of their localization.

In the experiment, double-exposure holograms were recorded for the fixed longitudinal displacement $\Delta l = (0 \pm 0.002)$ mm of the opaque screen for different curvatures of a spherical wave front of the radiation, used for scatterer illumination, chosen within the above range. The l_1 and l_2 values corresponded to the above presented. As an example, the interference patterns, localized in the imaging plane of the opaque screen, restricted by an image of the telescope pupil, are given in Fig. 6.

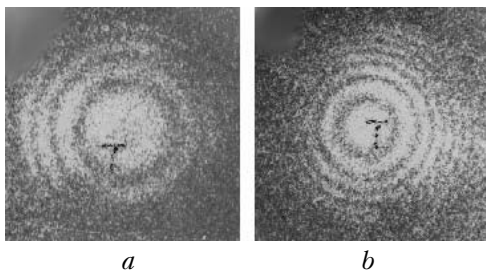


Fig. 6. Interference patterns localized in the scatterer-imaging plane and characterizing its longitudinal displacement in illuminating by radiation with divergent (a) and convergent (b) spherical waves.

They were recorded in the focal plane of a lens with $f_0 = 135$ mm in focal length when spatial filtering the diffraction field in the hologram plane by means of its retrieving with a small-aperture (≈ 2 mm) laser

beam. Figure 6a corresponds to the case of screen illumination by radiation with a divergent spherical wave ($R = 400$ mm) while Figure 6b is to the case of the convergent one ($R = 300$ mm). If the spherical wave radius satisfies the condition $780 \text{ mm} \leq |R| \leq \infty$, the zero order of interference exceeds $s = 9.6$ mm.

The interference pattern, localized in the hologram plane (see Fig. 5b), was recorded while reconstructing the hologram (Fig. 3) by a collimated beam of 50 mm in diameter with spatial filtration of the diffraction field in the focal plane of the lens L'_0 of 60 mm in diameter and 500 mm in focal length. In this case, the spatial extension of the interference pattern was equal to a calculated value of 43 mm. In addition, to retrieve the above interference pattern in case of recording the Fourier hologram at the stage of its retrieving, spatial filtration of the diffraction field in the frequency plane of the two-component optical system (Fig. 3) was necessary.

The value of the opaque screen longitudinal displacement was calculated for the known variables $\lambda, \mu, l, R, f_0, r_1,$ and r_2 for both the described and other interference patterns, recorded in the experiment; then it was compared with the known value. They agreed to each other up to 10% error, allowable in the experiment.

While two-exposure recording of the quasi-Fourier and Fourier holograms with a Galilean telescope to control transversal or longitudinal displacement of the scatterer the character of the interferometer sensitivity dependence on the enhancement of the Kepler tube sensitivity is different.¹ Hence, an analysis of the hologram recording according to Fig. 7, when the scatterer is in front of the telescope lens, is required.

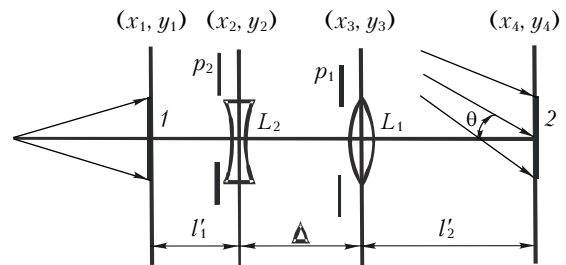


Fig. 7. Schematic view of two-exposure hologram recording.

In this case, the distribution of the complex amplitude of the field, corresponding to the first exposure, to the Fresnel approximation in the object channel in the photoplate plane is

$$\begin{aligned} \tilde{u}_1(x_4, y_4) \sim & \iiint \iiint t(x_1, y_1) \exp\left[\frac{ik}{2R}(x_1^2 + y_1^2)\right] \times \\ & \times \exp\left\{\frac{ik}{2l'_1}[(x_1 - x_2)^2 + (y_1 - y_2)^2]\right\} p_2(x_2, y_2) \times \\ & \times \exp\left[\frac{ik}{2f_2}(x_2^2 + y_2^2)\right] \exp\left\{\frac{ik}{2\Delta}[(x_2 - x_3)^2 + (y_2 - y_3)^2]\right\} \times \\ & \times p_1(x_3, y_3) \exp\left[-\frac{ik}{2f_1}(x_3^2 + y_3^2)\right] \times \end{aligned}$$

$$\times \exp\left\{\frac{ik}{2l_2'}[(x_3 - x_4)^2 + (y_3 - y_4)^2]\right\} dx_1 dy_1 dx_2 dy_2 dx_3 dy_3, \tag{41}$$

where l_1' is the distance between the opaque screen and the principal plane of the lens L_2 ; l_2' is the distance between the principal plane of the lens L_1 and the photoplate.

Based on the transforms, similar to those fulfilled in case when the scatterer was placed in front of the Galilean telescope lens, obtain the distribution of the field complex amplitude in the photoplate plane within the area of $D' \leq d_2 l' (l_2' + \mu\Delta) / (\mu l_1' l_2' + l\Delta)$ in diameter ($l' = l_2' + \mu\Delta + \mu^2 l_1'$) in the following form:

$$\begin{aligned} \tilde{u}_1(x_4, y_4) \sim & \exp\left[\frac{ik}{2r'}(x_4^2 + y_4^2)\right] \left\{ \tilde{F}(x_4, y_4) \otimes \right. \\ & \otimes \exp\left[-\frac{ik\mu^2 R}{2l'(\mu^2 R + l')}(x_4^2 + y_4^2)\right] \otimes \\ & \left. \otimes P_1'(x_4, y_4) \otimes P_2'(x_4, y_4) \right\}, \tag{42} \end{aligned}$$

where $r' = l'$ is the curvature of a divergent spherical wave; $\tilde{F}(x_4, y_4)$ is the Fourier transform of the function $t(x_1, y_1)$ with the spatial frequencies $\mu x_4 / \lambda l'$ and $\mu y_4 / \lambda l'$; $P_1'(x_4, y_4)$ is the Fourier transform of the telescope objective pupil function $p_1(x_3, y_3)$ with the spatial frequencies $x_4 / \lambda l_2'$ and $y_4 / \lambda l_2'$; $P_2'(x_4, y_4)$ is the Fourier transform of the telescope lens pupil function $p_2(x_2, y_2)$ with the spatial frequencies $\mu x_4 / \lambda(\mu\Delta + l_2')$ and $\mu y_4 / \lambda(\mu\Delta + l_2')$.

It follows from Eq. (42), that the quasi-Fourier transform of the transmission function of opaque screen 1 is formed in the plane of photoplate 2 (Fig. 7) within the area of D' in diameter, each point of which is extended up to the size of the subjective speckle, defined by the width of the function $P_1'(x_4, y_4) \otimes P_2'(x_4, y_4)$. In this case, the subjective speckle-field is superimposed with the phase distribution of a divergent spherical wave with the curvature $r' = l'$. In particular case of the scatterer illumination with a coherent radiation with a convergent spherical wave of l' / μ^2 in curvature, the distribution of field complex amplitude in the plane (x_4, y_4) corresponds to the Fourier transform of the function $t(x_1, y_1)$.

When the opaque screen is transversely displaced in its plane toward the x -axis to a , the distribution of the complex amplitude of the field, corresponding to the second exposure, in the object channel in the photoplate plane within the above area is defined as

$$\tilde{u}_2(x_4, y_4) \sim \exp\left[-\frac{ik(\mu^2 R + l')a^2}{2Rl'}\right] \times$$

$$\begin{aligned} & \times \exp\left(\frac{ik\mu a x_4}{l'}\right) \exp\left[\frac{ik}{2r'}(x_4^2 + y_4^2)\right] \times \\ & \times \left\{ \tilde{F}(x_4, y_4) \otimes \exp\left[-\frac{ik\mu^2 R}{2l'(\mu^2 R + l')}(x_4^2 + y_4^2)\right] \otimes \right. \\ & \left. \otimes \exp\left(-\frac{ik\mu a x_4}{l'}\right) \left\{ P_1'(x_4, y_4) \otimes P_2'\left[x_4 + \frac{(\mu^2 R + l')}{\mu R} a, y_4\right] \right\} \right\}. \tag{43} \end{aligned}$$

According to Eq. (43), the transversal displacement of the scatterer is accompanied by variation of the slope angle of subjective speckle-field to the value $\mu a / l'$ with respect to the speckle-field of the first exposure. In addition, a homogeneous displacement of the speckle-field component is observed there, caused by the diffraction of a plane wave on the pupil of Galilean telescope, to $(\mu^2 R + l')a / \mu R$.

If the double-exposure quasi-Fourier or Fourier hologram is recorded at the linear part of the photomaterial blackening curve with the use of a divergent spherical wave of $r' = l'$ in curvature, then the distribution of the complex amplitude of its transmittance, corresponding to the (-1) -st diffraction order, on the base of Eqs. (42) and (43) takes the form

$$\begin{aligned} \tilde{\tau}(x_4, y_4) \sim & \exp(-ikx_4 \sin\theta) \left\{ \tilde{F}(x_4, y_4) \otimes \right. \\ & \otimes \exp\left[-\frac{ik\mu^2 R}{2l'(\mu^2 R + l')}(x_4^2 + y_4^2)\right] \otimes P_1'(x_4, y_4) \otimes P_2'(x_4, y_4) + \\ & + \exp\left[-\frac{ik(\mu^2 R + l')}{2Rl'} a^2\right] \exp\left(\frac{ik\mu a x_4}{l'}\right) \times \\ & \times \left\{ \tilde{F}(x_4, y_4) \otimes \exp\left[-\frac{ik\mu^2 R}{2l'(\mu^2 R + l')}(x_4^2 + y_4^2)\right] \otimes \right. \\ & \left. \left. \otimes \exp\left(-\frac{ik\mu a x_4}{l'}\right) \left\{ P_1'(x_4, y_4) \otimes P_2'\left[x_4 + \frac{(\mu^2 R + l')}{\mu R} a, y_4\right] \right\} \right\} \right\}. \tag{44} \end{aligned}$$

If the diffraction field is spatially filtered while reconstructing the hologram in its plane on the optical axis (Fig. 2), and the phase change $(k\mu a x_4 / l') \leq \pi$ within the diameter of filtering aperture, then define the distribution of the field complex amplitude in the far focal plane of the lens L_0 as

$$\begin{aligned} \tilde{I}(x_5, y_5) \sim & \left\{ 1 + \cos\left(\frac{k(\mu^2 R + l')a^2}{2Rl'} + \frac{k(\mu^2 R + l')}{\mu R f_0} a x_5\right) \right\} \times \\ & \times \left| p_1\left(\frac{l_2'}{f_0} x_5, \frac{l_2'}{f_0} y_5\right) p_2\left(\frac{l_2' + \mu\Delta}{\mu f_0} x_5, \frac{l_2' + \mu\Delta}{\mu f_0} y_5\right) \right| \times \end{aligned}$$

$$\times t\left(-\frac{l'}{\mu f_0}x_5, -\frac{l'}{\mu f_0}y_5\right) \exp\left[\frac{ikl'(\mu^2R+l')}{2\mu^2Rf_0^2}(x_5^2+y_5^2)\right] \otimes \otimes P_0(x_5, y_5) \Big|^2. \tag{45}$$

It follows from Eq. (45) that to provide for the diffraction boundedness of the field by a telescope, the diameter D'_0 of the illuminated area of the scatterer at the stage of hologram recording should satisfy the condition $D'_0 \geq d_2l'/(l_2 + \mu\Delta)$. Then the subjective speckle structure is modulated by fringes, alternate on the x -axis, within the area $s' = d_2\mu f_0/(l_2 + \mu\Delta)$ of a telescope pupil image (here $l_2 < (\mu\Delta + l_2)$). In this case, the interferometer sensitivity depends both on the value and sign of the curvature of wave front of the coherent radiation, illuminating the scatterer while recording the hologram, due to a homogeneous displacement of the subjective speckle component, caused by the diffraction of a plane wave on the telescope pupil, in the hologram plane. The fringe period $\Delta\tilde{x}_5 = \lambda\mu Rf_0/(\mu^2R+l')a$ for positive R decreases with R due to the increase of the displacement of the above component of the subjective speckle, corresponded to the second exposure, in the hologram plane.

When the opaque screen 1 (Fig. 7) is illuminated with a coherent radiation with a convergent spherical wave, the fringe period increases with decreasing R in a range $(l'/\mu^2) \leq R \leq \infty$ up to infinity when $R = l'/\mu^2$; the Fourier transform of $t(x_1, y_1)$ is formed in the hologram plane; displacement of the speckles, corresponding to the second exposure, is absent. A further decrease of R results in enhancement of the interferometer sensitivity when recording the interference pattern, localized in the scatterer-imaging plane, due to occurrence and increase of a homogeneous displacement of the subjective speckle component, caused by the diffraction of a plane wave on the pupil of Galilean telescope, in the hologram plane. In contrast to Ref. 1, the interferometer sensitivity nonlinearly depends on the telescope magnification at $R \neq \infty$.

Let the spatial filtration of the diffraction field be performed on the optical axis in the scatterer-imaging plane (Fig. 3) when reconstructing the double-exposure quasi-Fourier hologram (phase change $[k(\mu^2R+l')a/\mu Rf_0] \leq \pi$), within the diameter of filtering aperture). Then the light distribution in the plane (x_6, y_6) of the hologram imaging with the unity magnification takes the form

$$\tilde{I}(x_6, y_6) \sim \left\{ 1 + \cos\left[\frac{k(\mu^2R+l')}{2Rl'}a^2 - \frac{k\mu ax_6}{l'}\right] \right\} \times \left| \tilde{F}(-x_6, -y_6) \otimes \exp\left[-\frac{ik\mu^2R}{2l'(\mu^2R+l')}(x_6^2+y_6^2)\right] \otimes P_0(x_6, y_6) \right|^2. \tag{46}$$

It follows from Eq. (46) that the subjective speckle-structure in the hologram-imaging plane is modulated with fringes of $\Delta\tilde{x}_6 = \lambda l'/\mu a$ in period. The fringe frequency depends on the hologram-plane scale of the Fourier transform of the function, characterizing the complex amplitude of scatterer transmittance or reflection.

Under control of longitudinal displacement of the opaque screen 1 (Fig. 7) in two-exposure hologram recording, the distribution of complex amplitude of the field, corresponding to the second exposure, in the object channel in the photoplate plane within an area of D' in diameter is defined as

$$\tilde{u}'_2(x_4, y_4) \sim \sim \exp(ik\Delta l) \exp\left[-\frac{ik\mu^2\Delta l}{2l'^2}(x_4^2+y_4^2)\right] \exp\left[\frac{ik}{2r'}(x_4^2+y_4^2)\right] \times \left\{ \tilde{F}'(x_4, y_4) \otimes \exp\left[-\frac{ik\mu^2(R-\Delta l)(l'+\mu^2\Delta l)}{2l'^2(\mu^2R+l')}(x_4^2+y_4^2)\right] \otimes \otimes P'_1(x_4, y_4) \otimes P'_2(x_4, y_4) \right\}, \tag{47}$$

where $\tilde{F}'(x_4, y_4)$ is the Fourier transform of the function $t(x_1, y_1)$ with the spatial frequencies $\mu x_4/\lambda l'(1 + \mu^2\Delta l/l')$ and $\mu y_4/\lambda l'(1 + \mu^2\Delta l/l')$.

If the double-exposure hologram is recorded at the linear part of the photo-material blackening curve with the use of a divergent spherical wave of $r' = l'$ in curvature, then the distribution of the complex amplitude of its transmittance, corresponding to the (-1)-st diffraction order, on the base of equations (42) and (47) takes the form

$$\tilde{t}'(x_4, y_4) \sim \exp(-ikx_4 \sin\theta) \times \left\{ \tilde{F}(x_4, y_4) \otimes \exp\left[-\frac{ik\mu^2R}{2l'(\mu^2R+l')}(x_4^2+y_4^2)\right] \otimes \otimes P'_1(x_4, y_4) \otimes P'_2(x_4, y_4) + \exp(ik\Delta l) \times \times \exp\left[-\frac{ik\mu^2\Delta l}{2l'^2}(x_4^2+y_4^2)\right] \times \times \left\{ \tilde{F}'(x_4, y_4) \otimes \exp\left[-\frac{ik\mu^2(R-\Delta l)(l'+\mu^2\Delta l)}{2l'^2(\mu^2R+l')}(x_4^2+y_4^2)\right] \otimes \otimes P'_1(x_4, y_4) \otimes P'_2(x_4, y_4) \right\} \right\}. \tag{48}$$

Let the spatial filtration of the diffraction field be performed on the optical axis in the hologram plane (Fig. 2) while retrieving the double-exposure hologram (phase change $[k\mu^2\Delta l(x_4^2+y_4^2)/2l'^2] \leq \pi$ within the filtering aperture diameter $\tilde{d}_f \leq \lambda l'(l_2 + \mu\Delta)/\mu^3 d_2 \Delta l$).

Then define the light distribution in recording plane 3 (Fig. 2) with accounting for the inequality $l'_2 < (\mu\Delta + l'_2)$ as

$$\begin{aligned} \tilde{I}'(x_5, y_5) \sim & \left\{ 1 + \cos \left[k\Delta l + \frac{k(\mu^4 R^2 - l'^2)\Delta l}{2\mu^2 R^2 f_0^2} (x_5^2 + y_5^2) \right] \right\} \times \\ & \times \left| p_2 \left(\frac{l'_2 + \mu\Delta}{\mu f_0} x_5, \frac{l'_2 + \mu\Delta}{\mu f_0} y_5 \right) t \left(-\frac{l'}{\mu f_0} x_5, -\frac{l'}{\mu f_0} y_5 \right) \right| \times \\ & \times \exp \left[\frac{ikl'(\mu^2 R + l')}{2\mu^2 R f_0^2} (x_5^2 + y_5^2) \right] \otimes P_0(x_5, y_5) \Big|^2. \quad (49) \end{aligned}$$

According to Eq. (49), a subjective speckle structure in the plane (x_5, y_5) of scatterer imaging, restricted by the image of Galilean telescope pupil, is modulated by fringes of equal slope – the system of concentric interference rings. In this case, the interferometer sensitivity is independent of the sign of a spherical wave curvature of the coherent radiation, used for scatterer illumination while recording the hologram, and has another character of the telescope magnification dependence in comparison with Ref. 1 at $R \neq \infty$. In addition, the interferometer sensitivity depends on the value of curvature R . Thus, when $|R|$ decreases within a range $(l'/\mu^2) \leq |R| \leq \infty$, the interferometer sensitivity decreases down to zero at $|R| = l'/\mu^2$. In this case, an additional slope of the subjective speckles, corresponding to the second exposure, in the hologram plane is invariable in Eq. (47) with respect to the similar ones of the first exposure. A further decrease of the spherical wave curvature results in enhancement of the interferometer sensitivity when recording the interference pattern, localized in the scatterer-imaging plane, due to occurrence and increase of a slope angle, radially varied from the optical axis, of the subjective speckles, corresponding to the second exposure, in the hologram plane.

In its turn, in case of double-exposure hologram retrieval with the spatial filtration of the diffraction field on the optical axis in the scatterer-imaging plane (Fig. 3) (phase change $\left[k(\mu^4 R^2 - l'^2)(x_5^2 + y_5^2) / 2\mu^2 R^2 f_0^2 \right] \leq \pi$ within the diameter of filtering aperture and the diameter $\tilde{d}_f \leq \lambda l'(l'_2 + \mu\Delta) / \mu^3 d_2 \Delta l$, when $f_{01} = l'/\mu$), the light distribution in the recording plane 3 (Fig. 3) takes the form

$$\begin{aligned} \tilde{I}'(x_6, y_6) \sim & \left\{ 1 + \cos \left[k\Delta l - \frac{k\mu^2 \Delta l}{2l'^2} (x_6^2 + y_6^2) \right] \right\} \times \\ & \times \left| \tilde{F}(-x_6, -y_6) \otimes \exp \left[-\frac{ik\mu^2 R}{2l'(\mu^2 R + l')} (x_6^2 + y_6^2) \right] \otimes P_0(x_6, y_6) \right|^2. \quad (50) \end{aligned}$$

According to Eq. (50), a subjective speckle structure in the plane (x_6, y_6) of hologram imaging is

modulated by fringes of equal slope – the system of concentric interference rings. In this case, the interferometer sensitivity depends on the hologram-plane scale of the Fourier transform of the function, characterizing the complex amplitude of scatterer transmittance and reflection, and increases with a decrease of the scale of Fourier transform $\tilde{F}(x_4, y_4)$.

Note, that in case of double-exposure recording of quasi-Fourier and Fourier holograms according to Fig. 7, the analysis of behavior dynamics of fringes in spatial filtering of the diffraction field exterior the optical axis gives results, similar to the case of hologram recording (Fig. 1).

In the experiment, double-exposure quasi-Fourier and Fourier holograms were recorded according to the scheme in Fig. 7 with the above parameters of Galilean telescope; distances l_1 and l_2 equaled to 150 and 200 mm, respectively, the curvature r' of a divergent spherical spatially restricted reference beam was 1122 mm. The opaque screen was longitudinally or transversely displaced before the second exposure by the same length as in case of hologram recording according to Fig. 1. In addition, the interference patterns, localized in the Fourier and hologram planes, were recorded similarly.

As an example, the interference patterns, localized in the Fourier plane and characterizing transversal displacement of opaque screen l (Fig. 7) are shown in Fig. 8.

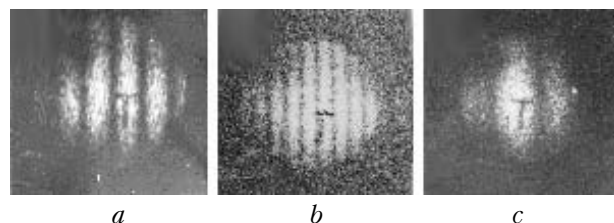


Fig. 8. Interference patterns localized in the plane of scatterer imaging and characterizing its transversal displacement under illuminating by a collimated beam (a), coherent radiation with divergent (b) and convergent (c) spherical waves ($R = 500$ mm).

The image of the opaque screen is restricted to the image of Galilean telescope pupil, for which $s' = 9$ mm corresponds to the calculated value.

In the above three cases (Fig. 8) and in other ones, connected with variation of the value and sign of curvature of a spherical wave of the radiation, illuminating the scatterer, the fringe periods were calculated for the known variables λ , a , μ , l' , R , and f_0 and compared with the measurement results. They agree to each other up to 10% error, allowable in the experiment.

A special case is realized in the experiment at $l'_1 = l_2$, $l'_2 = l_1$, and, hence, $l' = \mu^2 l$ and $D' \cong D$. As a result, the interference patterns, characterizing transversal or longitudinal displacement of the scatterer and localized in the hologram plane, were similar to those shown in Fig. 5. This also follows from Eqs. (17), (46) and (33), (50).

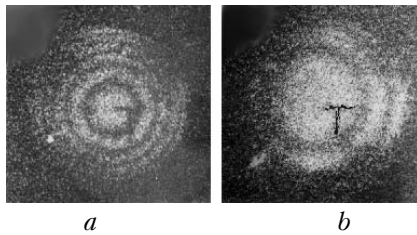


Fig. 9. Interference patterns localized in the plane of scatterer imaging and characterizing its longitudinal displacement under illuminating by radiation with divergent (*a*) and convergent (*b*) spherical waves.

The interference patterns in Fig. 9 characterize longitudinal displacement of opaque screen *l* (Fig. 7) and are localized in the Fourier plane; Figure 9*a* corresponds to the case when the scatterer is illuminated by the coherent radiation with divergent ($R=400$ mm) and Fig. 9*b* – with convergent ($R=300$ mm) spherical waves when recording the hologram. Both in these two cases and in others connected with variation of the value and sign of curvature of a spherical wave of the radiation, illuminating the scatterer when recording the hologram, the calculated value of longitudinal displacement of the opaque screen for the known λ , a , μ , l , R , f_0 , r_1 , and r_2 was compared with the known one. They agree to each other up to 10% error, allowable in the experiment.

Note, that double-exposure quasi-Fourier hologram recording according to the scheme in Fig. 7 at $R = \infty$ provides for the μ^2 -time enhancement of the interferometer sensitivity to the transversal scatterer displacement when recording the interference pattern, localized in the Fourier plane. This follows from comparison of Figs. 4*a* and 8*a* and Eqs. (12) and (45) and is explained by an increase of displacement of the subjective speckle component, caused by the diffraction of a plane wave on the pupil of Galilean telescope, in the hologram plane (see Eqs. (43) and (7)). Besides, the recording of the interference pattern, characterizing longitudinal scatterer displacement and localized in the Fourier plane, also provides for enhancement of the interferometer sensitivity at $R = \infty$. The μ^4 -time enhancement follows from comparison of Eqs. (49) and (30) and is explained by an increase of a slope angle, radially varied from the optical axis, of the subjective speckles, corresponding to the second exposure, with respect to the similar speckles of the first exposure.

Thus, the results of theoretical analysis of formation of interference patterns, characterizing transversal or longitudinal displacement of the scatterer in double-exposure recording of the quasi-Fourier and Fourier holograms with the use of a Galilean telescope along with performed experimental investigations have shown the following.

Similar to the case of Kepler tube, interference patterns are localized in two planes. Under control of transversal scatterer displacement for the interference pattern, localized in the Fourier plane of scatterer imaging, the interferometer sensitivity generally nonlinearly depends on telescope magnification and the sign of curvature of a spherical wave of the coherent radiation, used for scatterer illumination when recording the quasi-Fourier hologram.

For the interference pattern localized in the hologram plane, the interferometer sensitivity depends on the hologram-plane scale of the Fourier transform of the function, characterizing the complex amplitude of scatterer transmittance or reflection.

Under control of longitudinal scatterer displacement for the interference pattern, localized in the Fourier plane, the interferometer sensitivity in general has another character of power dependence on telescope magnification in comparison with a Kepler tube. For the interference pattern localized in the hologram plane, the interferometer sensitivity depends on the hologram-plane scale of the Fourier transform of the function, characterizing the complex amplitude of scatterer transmittance or reflection. In addition, an inhomogeneous displacement of the subjective speckles, corresponding to the second exposure, in the hologram plane with respect to similar speckles of the first exposure results in a displacement of the interference pattern center (the system of concentric rings), localized in both the Fourier and hologram planes, when spatial filtering the diffraction field exterior the optical axis. Because of the same reason, spatial filtration of the diffraction field in the Fourier plane is necessary to record the interference pattern, localized in the hologram plane, in case of double-exposure record of the Fourier hologram.

References

1. V.G. Gusev, Atmos. Oceanic Opt. **20**, No. 4, 325–339 (2007).
2. D. Goodman, *Introduction to Fourier Optics* (McGraw Hill, New York, 1968).
3. V.G. Gusev, Atmos. Oceanic Opt. **4**, No. 8, 558–564 (1991).
4. V.G. Gusev, Opt. Spektrosk. **76**, No. 3, 484–488 (1994).
5. M. Franson, *Speckle Optics* (Mir, Moscow, 1980), 165 pp.
6. L.M. Soroko, *Foundations for Holography and Coherent Optics* (Nauka, Moscow, 1971), 601 pp.
7. M. Born and E. Wolf, *Principles of Optics* (Pergamon, New York, 1959).
8. V.G. Gusev, Opt. Spektrosk. **72**, No. 4, 960–964 (1992).
9. R. Jones and C. Wykes, *Holographic and Speckle Interferometry* (Cambridge University Press, 1989).
10. E.B. Aleksandrov and A.M. Bonch-Bruевич, Zh. Tekhn. Fiz. **37**, No. 2, 360–369 (1967).
11. V.G. Gusev, Atmos. Oceanic Opt. **19**, No. 5, 407–416 (2006).
12. V.G. Gusev, Atmos. Oceanic Opt. **19**, No. 7, 575–585 (2006).